

Crustal architecture and tectonic evolution of the Gulf of Cadiz (SW Iberian margin) at the convergence of the Eurasian and African plates

Eulàlia Gràcia,¹ Juanjo Dañoibeitia,¹ Jaume Vergés, and Rafael Bartolomé²

Institut de Ciències de la Terra “Jaume Almera” (CSIC), Barcelona, Spain

Diego Córdoba

Departamento de Geofísica, Universidad Complutense de Madrid, Madrid, Spain

Received 1 November 2001; revised 27 June 2002; accepted 13 March 2003; published 16 July 2003.

[1] The Gulf of Cadiz, located at the southwestern Iberian margin, is characterized by widespread seismicity, compressional and strike-slip fault plane solutions and by a large, elongated positive free-air gravity anomaly, the Gulf of Cadiz Gravity High (GCGH). Multichannel seismic profiles across and along GCGH, together with bathymetric and gravity data, allow us to study in detail the tectonic architecture and crustal structure of the Gulf of Cadiz. The upper shelf and slope of the Gulf of Cadiz includes the main structural domains of the Betic fold and thrust belt. In the middle part of the Gulf, the Paleozoic basement crops out on the shallow Guadalquivir Bank and is associated with the largest signature of the GCGH, whereas toward the outer part of the Gulf, the basement deepens progressively. A large NW-SE normal fault and conjugate NE-SW faults define a prominent basement high associated with the GCGH. Modeling of the GCGH suggests localized crustal thinning of 10 km along the central part of the Gulf of Cadiz, probably generated during the Mesozoic rifting episode between the Iberian and African plates. Concentric wedges of fold and thrust belts and large allochthonous masses were emplaced in the Gulf of Cadiz during the Neogene compressional phase. The final emplacement of these units becomes progressively young from the SE (pre-early Langhian) toward the foreland in the NW (late Tortonian). Seafloor surface ruptures, pockmarks, and submarine landslides provide evidence of active faulting in the Gulf of Cadiz. To accommodate the present-day convergence between the African and Eurasian plates, previously extensional faults have probably been reactivated

and inverted at depth, as suggested by the intermediate depth seismicity. *INDEX TERMS*: 8105 Tectonophysics: Continental margins and sedimentary basins (1212); 3025 Marine Geology and Geophysics: Marine seismics (0935); 3040 Marine Geology and Geophysics: Plate tectonics (8150, 8155, 8157, 8158); 3010 Marine Geology and Geophysics: Gravity; 9325 Information Related to Geographic Region: Atlantic Ocean; *KEYWORDS*: swath bathymetry, multichannel seismic reflection, gravity anomalies, tectonics, Gibraltar Arc, Southwest Iberian Margin. **Citation**: Gràcia, E., J. Dañoibeitia, J. Vergés, R. Bartolomé, and D. Córdoba, Crustal architecture and tectonic evolution of the Gulf of Cadiz (SW Iberian margin) at the convergence of the Eurasian and African plates, *Tectonics*, 22(4), 1033, doi:10.1029/2001TC901045, 2003.

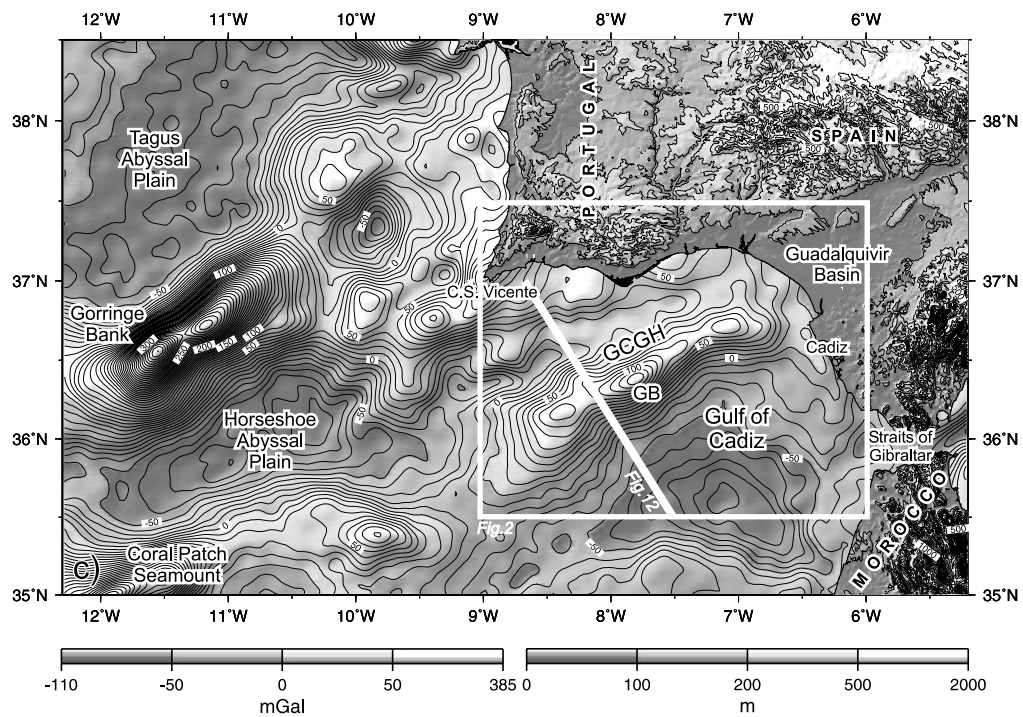
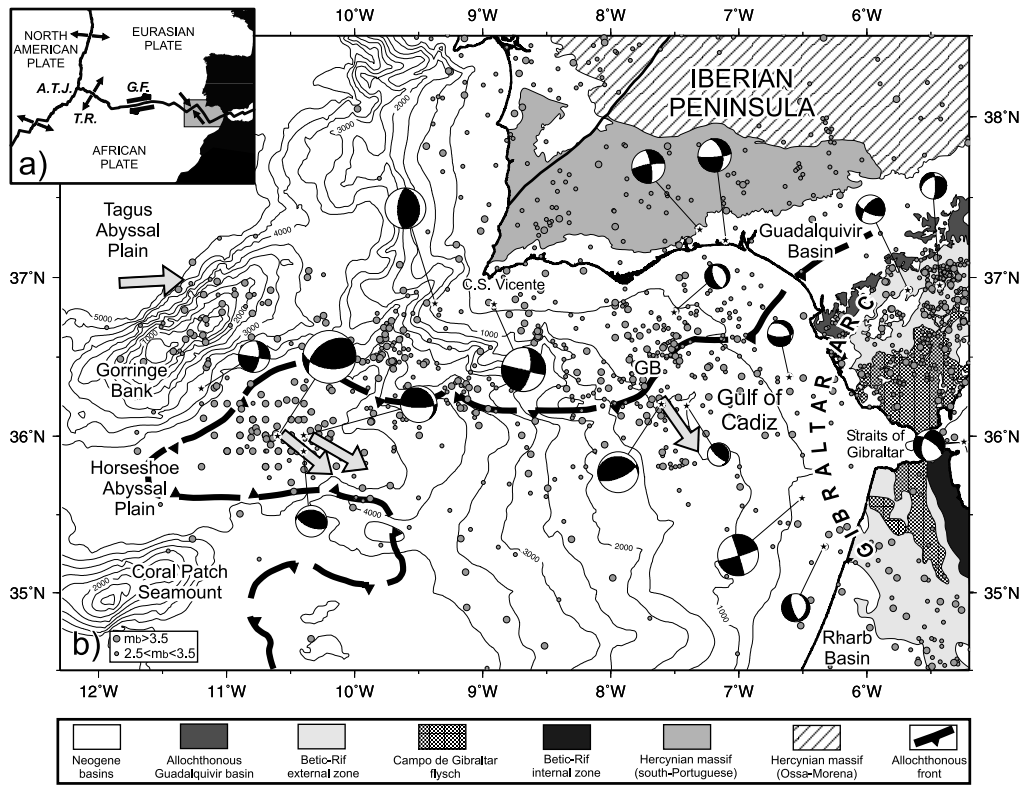
1. Introduction

[2] The Azores-Gibraltar seismic zone marks the present-day western boundary between the Eurasian and African plates [e.g., *Roest and Srivastava*, 1991; *Kiratzis and Papa-zachos*, 1995] (Figure 1a). Plate kinematic models together with focal mechanisms show that the motion between the two plates is slow (about 4 mm/yr) [*Argus et al.*, 1989] and mainly changes from a NE-SW extension along the Terceira Rift in the west, to an E-W right-lateral strike-slip along the Gloria fault [*Laughton et al.*, 1972] at the center, and a NW-SE compression and strike-slip in the east, from 14°W to the Straits of Gibraltar [e.g., *Minster and Jordan*, 1978; *Grimison and Chen*, 1986] (Figures 1a and 1b). The last segment, which corresponds to the eastern end of the Azores-Gibraltar zone, is characterized by a significant and diffuse seismic activity (Figure 1b), with events of $M_w = 8$ to 8.5 [*Fukao*, 1973; *Udias et al.*, 1976; *Grimison and Chen*, 1986; *Buforn et al.*, 1995]. In this area the plate boundary is not well defined, and the convergence between the African and European plates is accommodated through a widespread tectonically active deformation zone [e.g., *Sartori et al.*, 1994; *Hayward et al.*, 1999].

[3] *Tortella et al.* [1997] subdivided the area into two main morphotectonic domains: (1) the region between the Goringe Bank and Cape San Vicente to the west, and (2) the Gulf of Cadiz, between the Cape San Vicente and the Straits of Gibraltar to the east (Figure 1b). The first area is characterized by a complex and irregular topography,

¹Now at Unitat de Tecnologia Marina—CSIC, Centre Spain Mediterrani d'Investigacions Marines i Ambientals (CMIMA), Barcelona, Spain.

²Now at Institut Universitaire Européen de la Mer, UMR 6538 Domaines Océaniques, Plouzané, France.



dominated by large seamounts, deep abyssal plains, and massive rises [e.g., *Bergeron and Bonnin*, 1991; *Gràcia et al.*, 2003] (Figure 1b), such as the Gorringe Bank, where one of the largest amplitude gravity anomalies has been reported [e.g., *Souriau*, 1984] (Figure 1c). The oceanic convergence occurring in this area results in a continental collision as the plate boundary crosses toward the Straits of Gibraltar [*Grimison and Chen*, 1986], although the location of the ocean-continent boundary is still a matter of debate [*Hayward et al.*, 1999]. The second area, the Gulf of Cadiz, is underlain by Hercynian continental crust [*González et al.*, 1998] and is characterized by a smoother topography and by a prominent NE-SW trending positive free-air gravity anomaly [*Roberts*, 1970] (Figures 1b and 1c). The whole region has experienced a complex history since the Mesozoic in response to the changes in motion and location of the Eurasian-African plate boundary, jumping across the Iberian Peninsula [*Srivastava et al.*, 1990].

[4] Since the 1970s, the Gulf of Cadiz has been the subject of numerous geological and geophysical surveys, mostly tectonic and sedimentological work, with the aim of unraveling its complex geodynamic history [e.g., *Auzende et al.*, 1981] and hydrocarbon reservoir potential [e.g., *Delaplanche et al.*, 1982]. The main limitation of earlier studies in providing a complete picture of the Gulf of Cadiz structure is that they mainly focused on the shelf [*Malod and Didon*, 1975; *Flinch et al.*, 1996; *González et al.*, 1998; *Nelson and Maldonado*, 1999; *Lobo et al.*, 2000], or on isolated offshore seismic reflection profiles [e.g., *Malod and Mougenot*, 1979; *Banda et al.*, 1995; *Tortella et al.*, 1997].

[5] In this paper we present the results of a comprehensive multichannel seismic reflection (MCS) and high-resolution geophysical survey carried out in the Gulf of Cadiz, within the framework of the European BIGSETS project [*Mendes-Victor et al.*, 1999; *Zitellini et al.*, 2001]. This new data set together with previously acquired deep penetration seismic data [*Banda et al.*, 1995] comprise the totality of the Gulf of Cadiz, from the shelf to the outer part of the Gulf (6°W to 9°W) (Figures 1c and 2). The MCS profiles are strategically designed across and along the prominent positive free-air gravity anomaly, which henceforth will be termed the Gulf of Cadiz Gravity High (GCGH) (Figure 1c). The aims of the present paper are: (1) to provide new constraints on the

pattern and style of deformation of the Gulf of Cadiz shallow structure and on the timing of the main Cenozoic tectonic events, based on detailed interpretations of MCS profiles combined with high-resolution data, (2) to furnish new insights into the deep crustal structure across the Gulf of Cadiz, based on modeling of the gravity anomalies, and (3) to suggest a simple model relating the shallow and deep structure of the Gulf of Cadiz to the kinematic evolution of the southwestern Iberian margin.

2. Geological and Geophysical Setting of the Gulf of Cadiz: Overview

[6] The physiography of the Gulf of Cadiz is dominated by a NW-SE trending step-like morphology individualizing three main areas: (1) the shelf and talus, where most of the published high-resolution [*Malod and Mougenot*, 1979; *Baraza et al.*, 1999; *Rodero et al.*, 1999] and MCS surveys [*Flinch et al.*, 1996; *Maldonado et al.*, 1999] were carried out, (2) the middle part, dominated by the shallow Guadalquivir Bank (from 7°30'W to 8°W) and by a region referred to as “ridges and valleys” to the SE of the bank, and (3) the outer part (west of 8°W), dominated by spurs and large submarine canyons attaining a depth of more than 3000 m, such as the Portimao Canyon (Figure 2).

[7] The complex structure of the Gulf of Cadiz is a product of the interaction of the southern end of the Iberian rifted margin, the displacement of the Gibraltar Arc, and the convergence of the African and Eurasian plates [*Banda et al.*, 1995]. The original pattern of the Mesozoic Iberian rifted margin was partly obliterated during the successive deformation phases in the region [e.g., *Olivet*, 1996]. The Gibraltar Arc integrates the Betic and Rif mountain belts of Alpine Orogeny (Figure 1b), characterized by north, south and west vergent low-angle thrust systems with a radial tectonic transport [*Sanz de Galdeano*, 1990]. The offshore extension of the Western Betics, comprising the Guadalquivir Basin, the Betic External zones and the Campo de Gibraltar Flysch (Figures 1b and 2) was first identified in the Gulf of Cadiz by *Lajat et al.* [1975]. As a result of the Neogene convergence between the African and Eurasian plates, a number of allochthonous units were emplaced, and

Figure 1. (opposite) (a) Plate tectonic setting of the Southwest Iberian Margin (gray box), along the Azores-Gibraltar boundary between the Eurasian and African plates. ATJ: Azores Triple Junction; TR: Terceira rift; GF: Gloria fault. (b) Regional bathymetric map of the Southwest Iberian Margin (contour interval: 500 m) constructed from the predicted bathymetry of *Sandwell and Smith* [1997]. Seismicity from the *Instituto Geográfico Nacional* [1999] catalog for the period between 1965 and 1999 is depicted. Small gray dots are epicenters of earthquakes for $2.5 < m_b < 3.5$, and large gray dots are epicenters of earthquakes for $m_b > 3.5$. Fault plane solutions are from *Bufoorn et al.* [1988, 1995], *Ribeiro et al.* [1996], and *Mezcua and Rueda* [1997]. Light gray arrows show the direction of convergence (4 mm/yr) between the Eurasian and African plate from NUVEL1 model [*Argus et al.*, 1989]. Main geological domains of the Southwest Iberian Peninsula summarized from *Lanaja et al.* [1987] and *Frizon de Lamotte et al.* [1991]. Front of the allochthonous unit modified from *Torelli et al.* [1997]. (c) Subaerial topography and satellite-derived free-air gravity map of Southwest Iberia contoured at 100 m and 10 mGal intervals, respectively [*Sandwell and Smith*, 1997] (see also the United States Geological Survey Digital Elevation Model, USGS-GTOPO30, available at <http://edcdaac.usgs.gov/gtopo30/gtopo30.html>). Note the prominent NE-SW trending positive anomaly located along the Gulf of Cadiz, termed the Gulf of Cadiz Gravity High (GCGH). The white outlined box depicts the study area presented in Figure 2. The location of the profile modeled in Figure 12 is depicted by a thick white line. GB: Guadalquivir Bank.

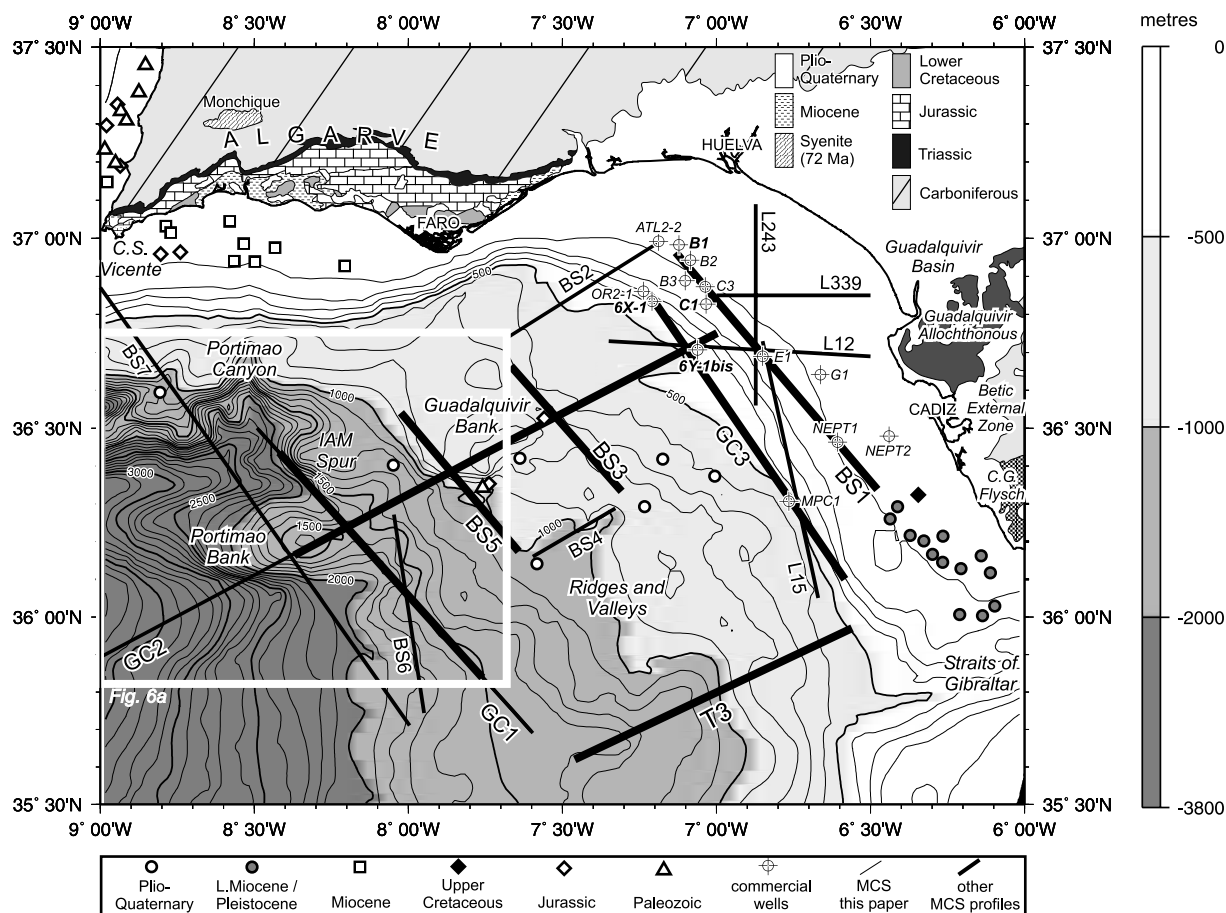


Figure 2. Bathymetric map of the Gulf of Cadiz (contour interval: 100 m) and main geological units onshore modified from *Frizon de Lamotte et al.* [1991] and *Terrinha* [1998]. All seismic reflection profiles used for this study are depicted. They comprise recently acquired data from the BIGSETS project (“BS” profiles); deep-seismic reflection data from the IAM project available for this work (“GC” and T3 profiles) [Banda *et al.*, 1995; Tortella *et al.*, 1997]; and seismic reflection profiles published by Maldonado *et al.* [1999] (“L” profiles). The multichannel seismic reflection (MCS) profiles presented in this paper are depicted as bold lines. Locations of commercial wells [Lanaja *et al.*, 1987] and results from dredges and shallow cores are also depicted [Baldy *et al.*, 1977; Malod and Mougnot, 1979]. The white outlined box depicts the area presented in Figure 6a. L. Miocene: Late Miocene; CG Flysch: Campo de Gibraltar Flysch.

these have been identified from the Gulf of Cadiz to the Horseshoe Abyssal Plain [Bonnin *et al.*, 1975; Torelli *et al.*, 1997; Flinch *et al.*, 1996; Maldonado *et al.*, 1999; Somoza *et al.*, 1999] (Figure 1b). The origin and different emplacement mechanisms of these allochthonous units are still controversial, and will be discussed at the end of this paper.

[8] Roberts [1970] first identified the large GCGH free-air anomaly, which poorly correlates with the seafloor topography (Figures 1b and 1c). Magnetic data depict a more complicated pattern [Dañobeitia *et al.*, 1999] although both potential-field data show the highest amplitudes in the middle of the Gulf of Cadiz. Thus, in the proximity of the Guadalquivir Bank, free-air gravity anomalies locally exceed 130 mGal [Roberts, 1970], and magnetic anomalies reach up to 300 nT peak-to-peak

[Dañobeitia *et al.*, 1999]. Deep MCS and wide-angle seismics from the IAM project [Banda *et al.*, 1995] (1) allowed the recognition of the main tectonosedimentary units of the SW Iberian Margin [Tortella *et al.*, 1997], (2) revealed the continental nature of the Gulf of Cadiz crust, and (3) provided evidence of a progressive crustal thinning from the SW Iberian shelf to the middle of the Gulf [González *et al.*, 1996, 1998].

3. Data and Methods

[9] This study presents an integration of different types of data: MCS, high-resolution bathymetry, subbottom profiler, and gravity. The main dataset comprises a series of seven MCS profiles (BS1 to BS7) acquired in the Gulf of Cadiz

within the framework of the BIGSETS project (BIGSETS cruise, R/V *Urania*, November 1998) [Gràcia *et al.*, 2000; Zitellini *et al.*, 2001] (Figure 2). The data were collected using a 48-channel, 3 km long streamer and a 1000 cubic inches Sodera-SSI-airgun array. The airguns were fired every 10, 15 and 40 s. The speed of the ship was 4.5–5 knots, yielding a shot spacing of about 25, 37.5 and 100 m, respectively. The processing sequence for these data included deconvolution before stack, band-pass filtering, velocity analysis and normal moveout correction before stacking. An f-k migration with a constant velocity of 1700 m/s (profiles BS1 and BS3), and a Kirckhoff migration (profile BS5) were also performed. The profiles depicted here, BS1, BS3 and BS5 trend NW-SE (Figure 2) perpendicular to the main orientation of GCGH.

[10] Additional MCS data are available in the area. They consist of four deep MCS profiles (GC1, GC2, GC3 and T3) acquired in 1993 in the framework of the IAM project (Figure 2). For details on acquisition and processing, see Banda *et al.* [1995]. Profiles GC1 and GC3 are arranged across the GCGH, whereas GC2 runs along the maximum values of the gravity anomaly. Profile T3 runs parallel to the GCGH, about 95 km to the southeast (Figure 2). The original IAM profiles, with a record length of up to 14 s TWTT [Tortella *et al.*, 1997], were reprocessed, plotted on the same scale as the BIGSETS lines (0 to 4s–5s TWTT) and reinterpreted in the light of the new data.

[11] During a subsequent cruise of the BIGSETS project (PARSIFAL cruise, R/V *Hesperides*, May 2000), swath bathymetry (Simrad EM12), high-resolution (2–5.5 kHz) TOPAS subbottom profiles, and gravity data were collected in the outer part of the Gulf of Cadiz (from 7°30'W to 9°W), and will also be presented here (Figure 2).

4. Tectonic and Gravity Structure of the Gulf of Cadiz

[12] Lithostratigraphy of the seismic units recognized on the MCS profiles was established on the basis of several published nearshore oil exploration wells [Lanaja *et al.*, 1987] (Figures 2 and 3). The following units were distinguished (Figure 3): (1) Paleozoic basement, mainly composed of shales, coal and volcanic rocks, which on the MCS records are characterized by discontinuous, high-amplitude, low-frequency hyperbolic facies, (2) Triassic evaporites (anhydrite and gypsum), imaged by reflectors of variable amplitude and frequency, showing diapiric structures on the MCS profiles, (3) Jurassic to early Cenozoic units, mostly composed of limestones, marls and dolomites with low-amplitude, highly reflective discontinuous seismic facies, (4) late Miocene unit, termed the Guadalquivir Allochthonous unit [Berástegui *et al.*, 1998], which consists of a mixture of Triassic gypsum and clays with incoherent bedding enclosing blocks of heterogeneous lithologies of Triassic, Upper Cretaceous and Paleocene age [e.g., Maldonado *et al.*, 1999]. This unit is characterized by high-frequency, high-amplitude, discontinuous hyperbolic facies, which hinders imaging of underlying seismic units, and (5) a thick Plio-Quaternary unit composed of silty clays

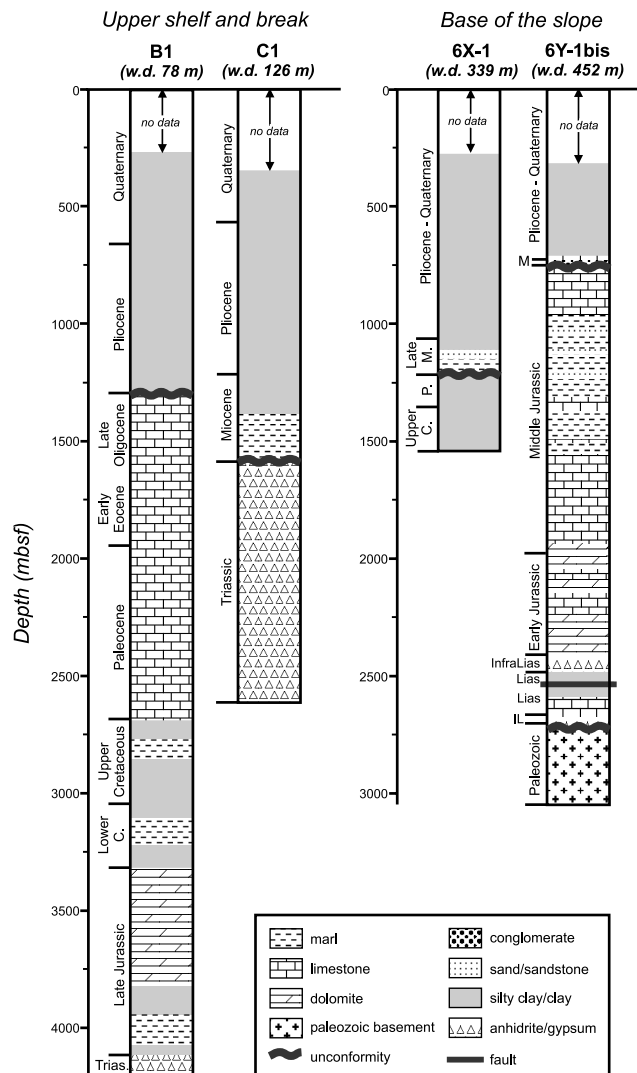
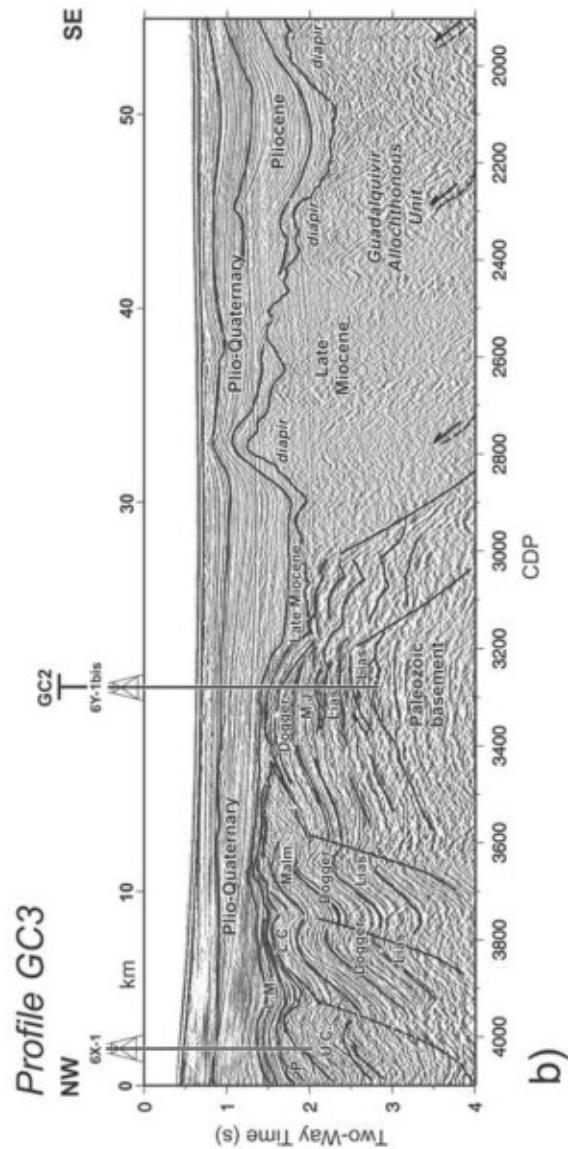
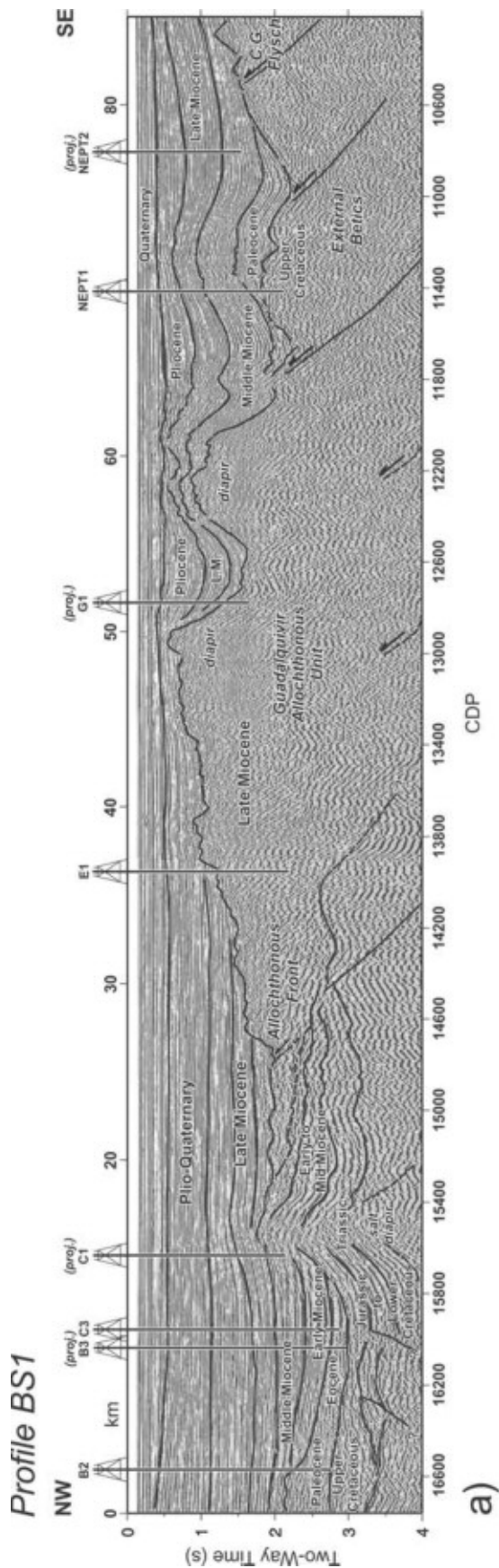


Figure 3. Simplified lithologic logs of the most representative commercial wells used for stratigraphic correlation between the MCS shelf profiles and the rest of MCS profiles (see location in Figure 2). Trias: Triassic; IL: InfraLias; C: Cretaceous; P: Paleocene; M: Miocene; wd: water depth; mbsf: meters below seafloor. Modified from Lanaja *et al.* [1987].

and clays imaged by well stratified reflectors with high-frequency, low-amplitude and very good lateral continuity.

4.1. Structure of the Inner Part of the Gulf of Cadiz: Betic Fold and Thrust Belt

[13] The inner part of the Gulf of Cadiz is characterized by an arc-shaped shelf, about 45 km wide and 130 m deep, and a narrow and steep slope, with its base limited by the 500 m isobath (Figure 2). The geometry of this part of the Gulf of Cadiz is well illustrated by profiles BS1 and GC3 (Figure 4). From top to bottom, both MCS profiles are arranged in a well-stratified upper sedimentary unit overlying a regional unconformity with a rough topography.



The upper sedimentary unit shows a clear lateral variability: To the northwest, the unit is thick, relatively undisturbed, corresponding to the submarine continuation of the foreland Guadalquivir Basin, whereas to the southeast, it is characterized by anticlinal and synclinal structures, corresponding to the continuation of the Betic fold and thrust system observed onland [e.g., *Berástegui et al.*, 1998] (Figure 4).

[14] In its thickest part, the foreland basin is composed of stratified units dating from early Miocene to Quaternary, based on wells C3 and B3 (Figures 2 and 4a). On profile GC3, the geometry of this infill shows an onlap of late Miocene sediments above the regional unconformity, as deduced from its geometry and oil well 6X-1 (Figures 3 and 4b). The structure underneath the foreland basin is characterized by a system of SE verging folds and thrusts, composed of highly reflective seismic units of Paleozoic/Mesozoic to early Tertiary age (Figures 3 and 4b). Oil well 6Y-1bis reaches the top of the Paleozoic basement at 3500 m below sea level at CDP 3300 of line GC3 (Figures 3 and 4b). The Mesozoic to early Tertiary units beneath the foreland basin are tilted toward the northwest, with a progressive shallowing of the older units to the southeast. Their contact with the fold and thrust belt is sharp, steeply dipping toward the southeast (CDPs 2800 to 3000 in Figure 4b), probably following the fault surface of a basement and Mesozoic tilted block.

[15] The front of the Betic fold and thrust system is located around CDPs 15500 and 3100 in profiles BS1 and GC3, respectively. On profile BS1, the front overthrusts early to middle Miocene strata, deformed by a diapiric structure probably composed of Triassic evaporites. On line GC3, the front slightly folds late Miocene deposits (Figure 4). A thick sedimentary succession, dating from late Miocene to Quaternary, onlaps the frontal paleotopography of the fold and thrust system reaching a maximum height at CDP 12900 of line BS1 (Figure 4a). From there and toward the southeast, the geometry of the fold and thrust belt shows growth synclines between paleohighs, with axes at CDPs 12600, 11700, and 11000 in profile BS1. The synclines show a progressive thinner and younger growth infill toward the northwest, ranging from early-middle Miocene to late Miocene-Pliocene based on well stratigraphy [*Lanaja et al.*, 1987] (Figure 4a). On line GC3, the entire syntectonic infill succession is gently tilted to the northwest, onlapping a significant paleohigh toward the southeastern end of the profile. Quaternary units are subhorizontal, suggesting that deformation mostly stopped before their deposition.

4.2. Structure of the Middle Part of the Gulf of Cadiz: Guadalquivir Bank

[16] The middle part of the Gulf of Cadiz is dominated by the prominent Guadalquivir Bank, a 28 km long, 12 km

wide feature cropping out at the seafloor at 550 m depth, as observed on the bathymetric map (Figure 2). The geometry across this part of the Gulf is imaged along profiles BS3, located northeast of the bank, and BS5, across the steepest slopes of the Guadalquivir Bank (Figure 5).

[17] Profile BS3 shows a general internal disposition similar to that of the shelf profiles BS1 and GC3 (Figure 5a), i.e., a thick, relatively undisturbed Neogene to Quaternary succession at the front of the fold and thrust belt, and a system of growth anticlines and synclines to the southeast. In the foreland, the Miocene to Pliocene units display a significant tilt toward the northwest, where they show erosional surfaces (Figure 5a). These units partly onlap the Guadalquivir Allochthonous thrust front, which shoals considerably toward the center of the profile (CDPs 1800 to 2200, in Figure 5a). These Neogene tilted units constitute the northwestern flank of a wide antiform, probably active after the emplacement of the allochthonous. The southeastern flank of this antiform shows small wavelength anticlines and synclines, which might also have been active recently, as evidenced by the Pliocene and Quaternary growth-strata (Figure 5a). These folds developed on top of the Mesozoic and Tertiary units constituting the NW vergent fold and thrust belt of the External Betics. The frontal thrust describes a low-angle trajectory between CDPs 1200 to 1800, from where it dips toward the southeast. This prominent feature probably reactivates a previously normal fault deforming the Paleozoic and Mesozoic cover, as observed on the shelf (Figures 4b and 5a).

[18] The MCS profile BS5 crosses the Guadalquivir Bank at CDP 2200 (Figure 5b) and follows a structural configuration similar to the earlier profile. The Neogene sedimentary units are also arranged following an antiformal structure, interrupted by the outcrop of the Guadalquivir Bank (Figure 5b). Dredges at the southern flank of the Guadalquivir Bank recovered rocks of Paleozoic age [*Malod and Mougnot*, 1979] (Figure 2). The Guadalquivir Bank is bounded to the NW by several small-throw normal faults, and to the SE by a large normal fault, displacing the top of the hanging wall block by several hundred meters (Figure 5b). North of the bank, well-stratified Miocene to Pliocene units are tilted toward the northwest, onlapping into Paleogene and Mesozoic units. At CDP 1900, the most recent sedimentary units are cut by small-throw, closely spaced SE dipping normal faults, suggesting active faulting (Figure 5b). Pockmarks, first described along the shelf area [*Baraza et al.*, 1999] are also commonly observed at this flank of the bank affecting the uppermost sedimentary units (Figure 6b). They seem to be formed by pore-water or gas seepage associated with active faulting [*Harrington*, 1985].

Figure 4. (opposite) (a) Interpreted MCS profiles BS1 and b) GC3. Both profiles are located along the Gulf of Cadiz shelf. MJ: Middle Jurassic; LC: Lower Cretaceous; UC: Upper Cretaceous; P: Paleocene; M: Miocene; CG Flysch: Campo de Gibraltar flysch. Paleozoic basement is depicted in dark green, Mesozoic to Paleogene units are in light green, and Neogene units in yellow. The Guadalquivir Allochthonous unit is depicted in red, and the Campo de Gibraltar and External Betics in brown. Faults are depicted in black, in dashed line when inferred. Same legend applies for Figures 5, 7, and 8. See color version of this figure at back of this issue.

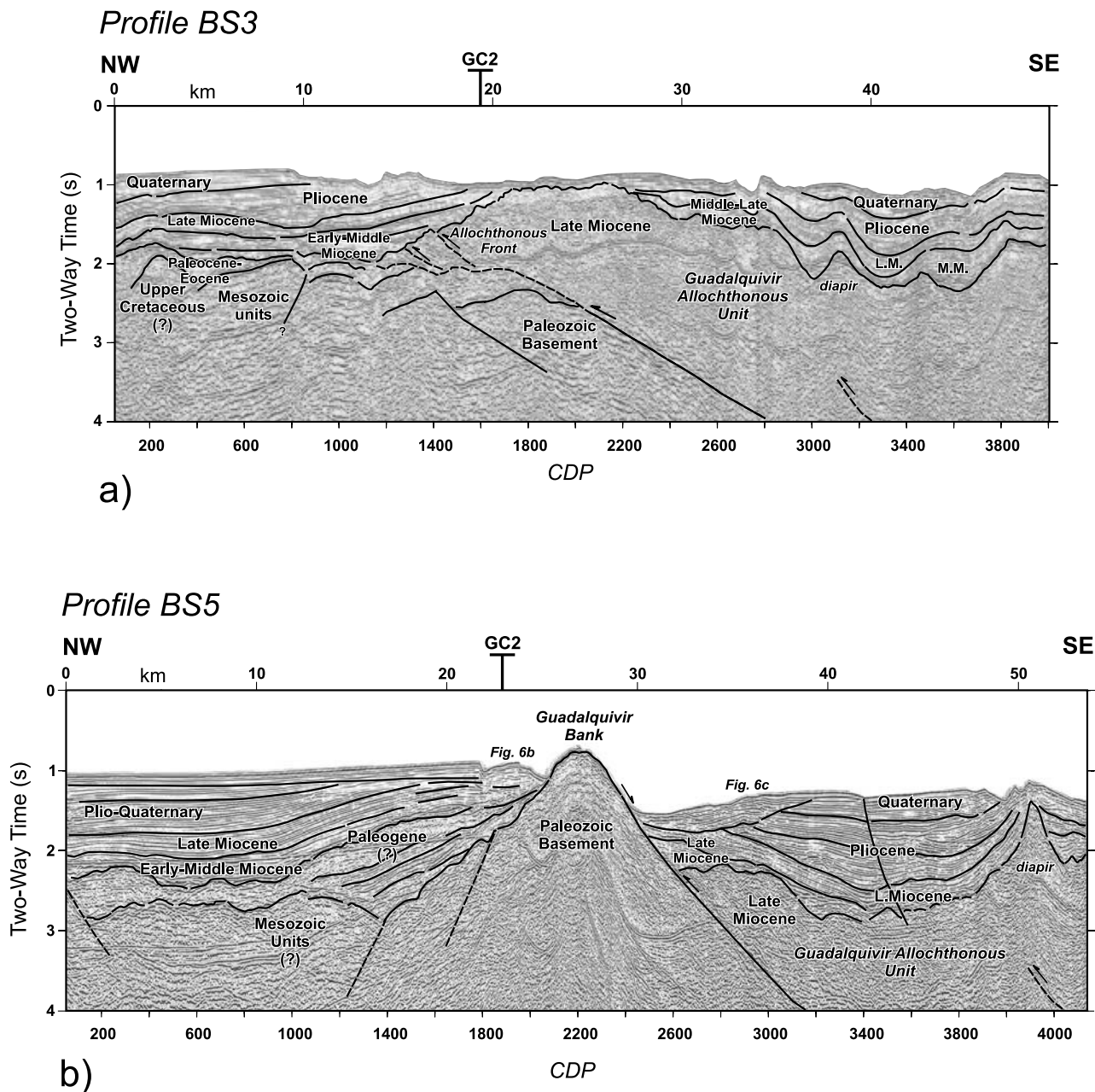
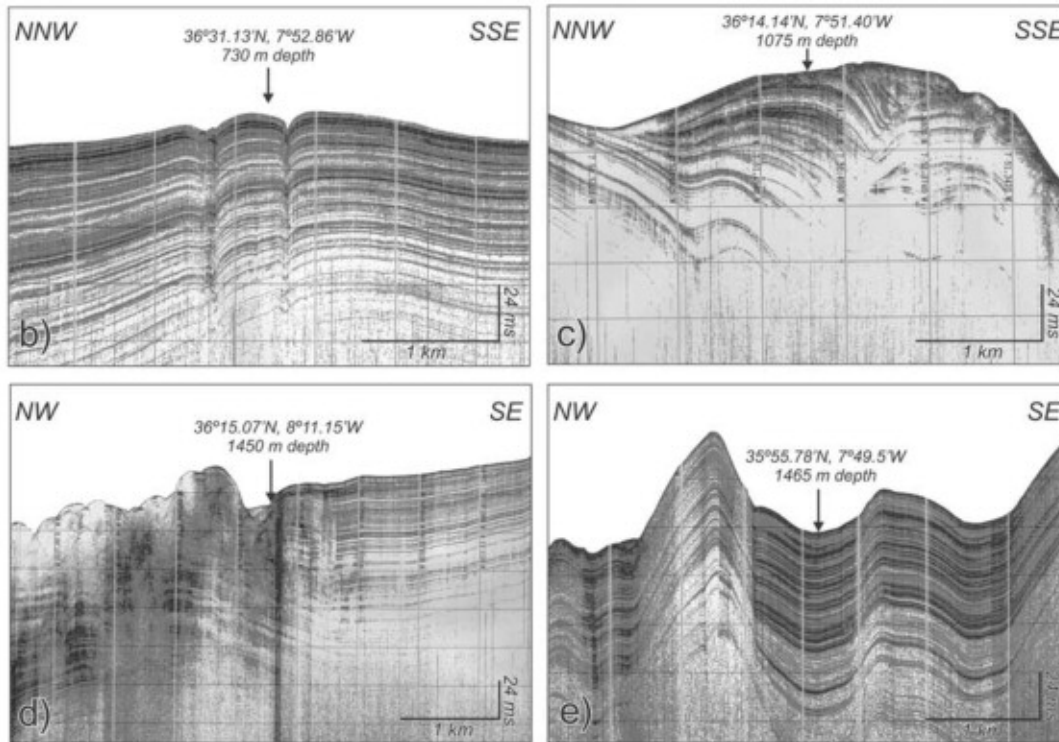
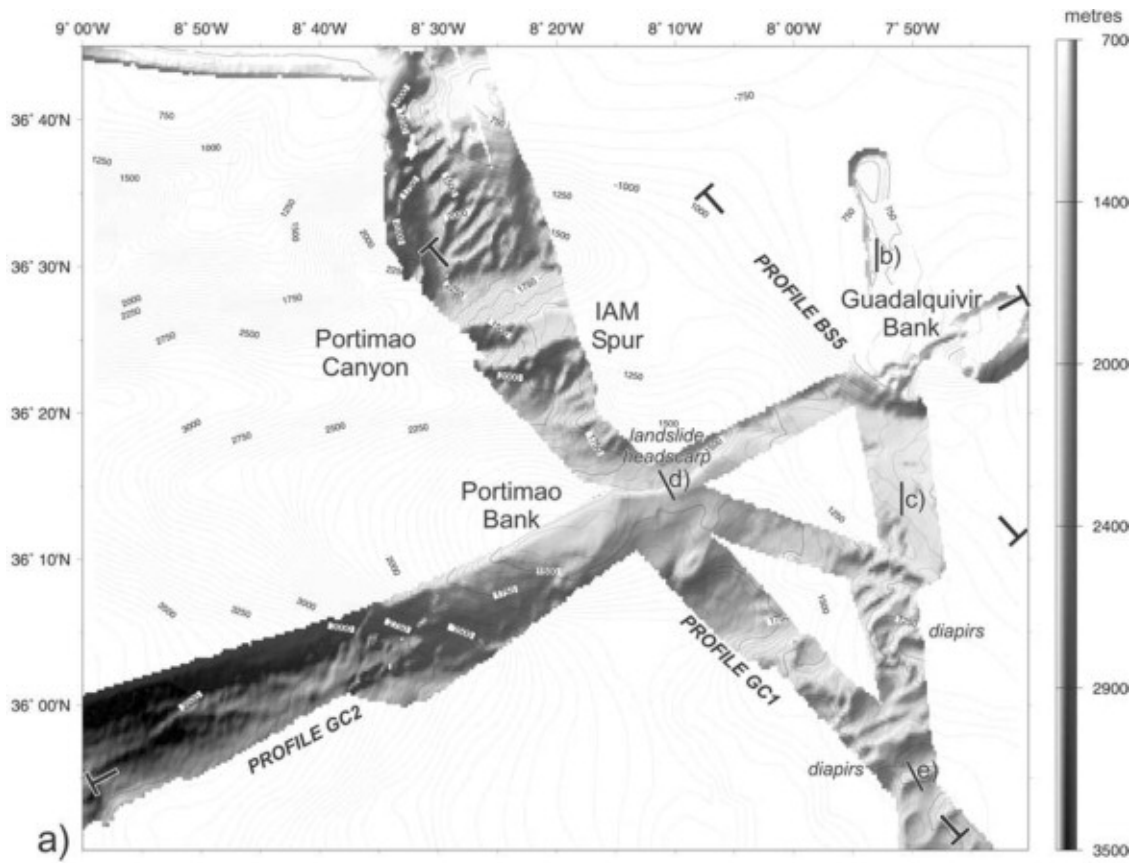
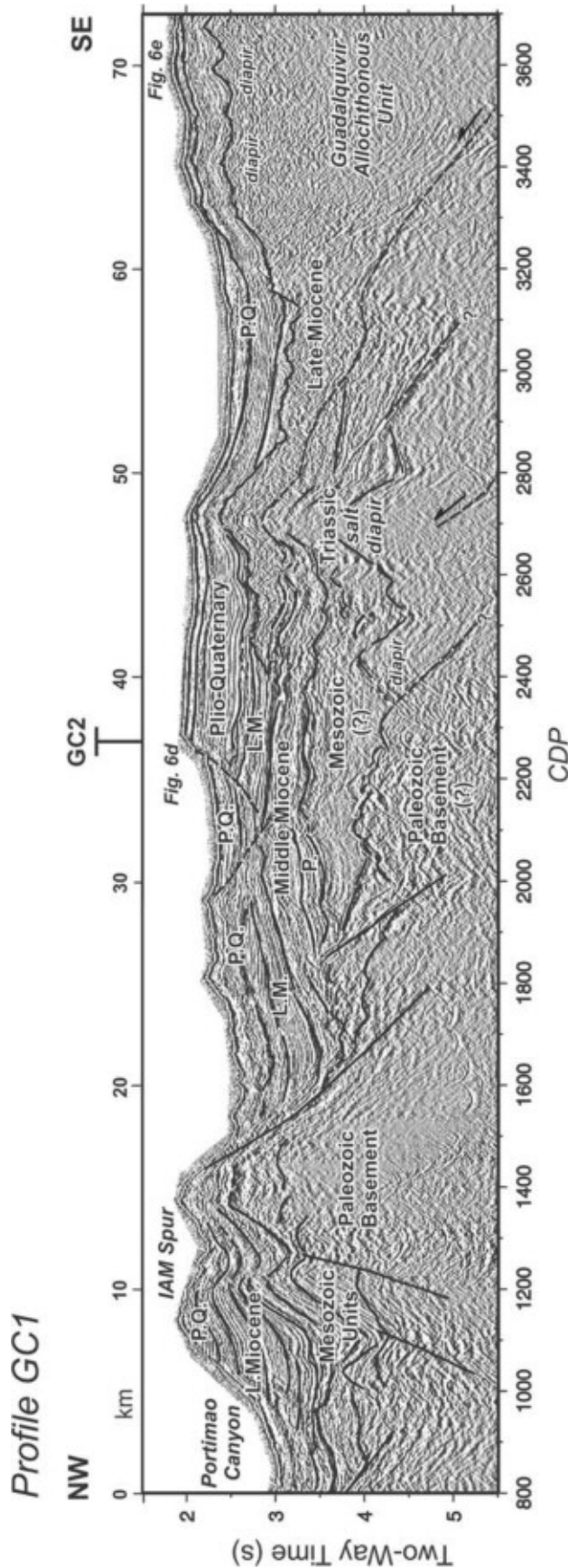


Figure 5. (a) Interpreted MCS profiles BS3 and (b) BS5. Both profiles are located in the middle of the Gulf of Cadiz, around the Guadalquivir Bank. LM: Late Miocene; MM: Middle Miocene. Location of Figures 6b and 6c are depicted on profile BS5. See color version of this figure at back of this issue.

Figure 6. (opposite) (a) Newly acquired bathymetric swaths superimposed onto preexistent bathymetry of the middle part of the Gulf of Cadiz (contour 50 m). The main physiographic features and multichannel seismic reflection profiles are located. A selection of four high-resolution subbottom profiles, depicted by short black lines (b to e), are presented here: (b) Pockmarks affecting the uppermost sedimentary layers, north of the Guadalquivir Bank; (c) Gentle folding of the upper sedimentary units south of the Guadalquivir Bank; (d) Landslide deposit, characterized by a chaotic acoustic facies, at the foot of a curved headscarp; (e) Diapiric structures affecting parallel-bedding sedimentary units. Latitude, longitude, and water depth in the center of each image (tip of the arrow) are given.





[19] To the southeast of the basement high, at the base of the stratified units, the Guadalquivir Allochthonous unit shows diapiric structures (CDP 4000). The overlying late Miocene units are folded showing a synclinal geometry, and are overlapped by Plio-Quaternary units. This thick sedimentary infill is cut by a small-throw SE dipping steep normal fault, located around CDP 3600. The Plio-Quaternary sedimentary units located at the foot of the bank show contourite-bedding and major channel incisions (Figures 5b and 6c), probably generated by the outflow currents of the Mediterranean Bottom Water, from the Straits of Gibraltar to the Atlantic oceanic basins [Nelson *et al.*, 1993].

4.3. Structure of the Outer Part of the Gulf of Cadiz: Portimao Bank

[20] The outer part of the Gulf of Cadiz is characterized by a very rough topography, dominated by large submarine canyons that are deeply incised in platformal areas or spurs (Figure 6a). The MCS profile GC1 runs across this part of the Gulf (Figure 7). To the northwest of this profile, we recognized the NW tilted narrowly folded and faulted Mesozoic cover. It is overlain by a 1.3 s TWTT thick late Miocene and Plio-Quaternary succession, also tilted to the northwest and strongly eroded. The whole succession is bounded by the erosional Portimao Canyon to the north, and by a large SE dipping normal fault to the south, individualizing a structural high termed the IAM Spur (Figure 7). At the center of the profile, the Miocene sedimentary units are folded, arranged in a large and wide anticline, as also observed on lines closer to the shore. They are overlain by a subhorizontal Plio-Quaternary succession. The entire Neogene to Quaternary succession is deformed by small-throw normal faults, such as the conjugate faults near CDP 2200, which may accommodate present-day deformation. The chaotic facies observed at the base of one of these fault scarps (Figure 6d) probably corresponds to slope instability deposits, supporting the idea of recent tectonic activity.

[21] In the central part of the profile, the Paleozoic basement is found at greater depths, at about 1.6 s TWTT below the seafloor (Figure 7). Above this basement, the Mesozoic cover shows diapiric structures probably cored by Triassic evaporites. The front of the Guadalquivir Allochthonous unit, located between CDPs 2400 and 2800, is affected by one of these diapirs. Toward the southeastern end of the profile, the allochthonous unit also shows diapiric structures, deforming up to the Quaternary strata (Figures 6e and 7). On the seafloor, the emerging diapirs tend to form small ridges, such as the ones identified on the swath bathymetry map (Figure 6a).

4.4. Structure Along the Gulf of Cadiz

[22] Two longitudinal MCS profiles (GC2 and T3) cut across the previously described profiles and structures, from

Figure 7. (opposite) Interpreted MCS profile GC1 in the outer part of the Gulf of Cadiz, south of the Portimao Canyon. P: Paleocene; LM: Late Miocene; PQ: Plio-Quaternary. Location of Figures 6d and 6e are depicted. See color version of this figure at back of this issue.

the shelf to the outer part of the Gulf of Cadiz (Figures 2 and 8). Profile GC2 clearly images the arrangement of the Paleozoic basement and Mesozoic cover, which follows a horst and graben geometry along the Gulf of Cadiz. From NE to SW, three main basement highs are individualized, termed A, B and C, respectively (Figure 8a). High A is located at the intersection between profiles GC2 and GC3, at 3500 m depth, cored by oil well 6Y-1bis (Figures 4b and 8a). Toward the center of the profile, the Paleozoic basement shallows progressively until cropping out at the Guadalquivir Bank (High B) at CDP 3300 (Figure 8a), located near the intersection with profile BS5. From there, the basement deepens progressively, following a SW dipping staircase of normal faults, in correlation with a significant increase in water depth. High C, termed the Portimao Bank, is located at the end of the profile (CDP 5200, 2.5s TWTT) (Figure 8a). A lens-shaped section of the Guadalquivir Allochthonous unit is observed at profile GC2 (CDPs 800 to 2500), confined between Highs A and B. We can clearly observe its maximum thickness of 1.6 s TWTT at CDP 1700 (Figure 8a). Overlying the previously described units, a thick sedimentary sequence composed of slightly deformed Neogene and Plio-Quaternary units is observed (Figure 8a).

[23] Profile T3 complements the previously presented MCS data as it runs along the southern part of the Gulf of Cadiz. At the northeastern end of this profile, near the shelf, we recognize the thrusting geometries of the Campo de Gibraltar Flysch and External Betics units. The Guadalquivir Allochthonous unit is continuously imaged from CDP 2600 as far as the southwestern end of this profile. Some of the diapirs of this unit reach the seafloor, deforming the overlying stratified Neogene and Plio-Quaternary units. Active mud volcanoes have been identified in this part of the Gulf [Gardner, 2001]. The Paleozoic basement and Mesozoic cover are not observed along this profile, as they are probably at greater depths than the 0–5 s TWTT window imaged here (Figure 8b).

4.5. Free-Air Gravity Signature at the Gulf of Cadiz

[24] The large NW-SE trending positive anomaly termed the Gulf of Cadiz Gravity High (GCGH) (Figure 1c) seems to be related to a narrow, elongated basement high running along the central part of the Gulf. When seen in detail, the GCGH is composed of the alignment of three local gravity highs, corresponding to the individual structural highs (A, B and C) identified on the MCS profiles (e.g., Figure 8a).

[25] The first of these highs (High A) corresponds to a local maximum of the gravity anomaly (<100 mGal) (profile GC3, Figure 9). Nearshore, the gravity anomaly abruptly decreases in amplitude, defining the NE termination of the basement high around 6°30'W (Figure 1b). The highest values (120 mGal) are recorded near the outcrop of the Guadalquivir Bank (High B), probably resulting from the topography effect (profile BS5, Figure 9). The third high, the Portimao Bank (High C), is characterized by a local 100 mGal gravity anomaly (profile BS7, Figure 9). The southwestern boundary of the basement high is defined by a progressive decrease in the gravity anomaly amplitude around 9°W (Figure 1b).

[26] The northern flank of the GCGH is separated from the Algarve margin by a gentle gravity low, whereas its southern flank is associated with a very steep gravity gradient (Figure 1c). South of the GCGH, there is a large decrease in the free-air gravity anomalies, up to –100 mGal (profile T3, Figure 9), which probably correlates with a progressive deepening of the Paleozoic basement (Figure 8b).

5. Discussion

5.1. Synthesis of the MCS and Gravity Data: Structural Map of the Gulf of Cadiz

[27] The joint interpretation of the MCS profiles and gravity data was summarized on the structural map of the Gulf of Cadiz, which shows (1) the geometry of the basement and cover, and (2) the extent and contacts of the allochthonous units (Figure 10).

[28] Three prominent basement highs, associated with the GCGH, extend about 225 km along the center of the Gulf of Cadiz. They are controlled by two main structural trends of normal faults: (1) a large NE-SW trending fault, which we termed the Guadalquivir Fault, defining the southeastern flank of the basement high and correlated with a steep gradient in the gravity signature; and (2) a number of short NW-SE trending faults, individualizing the three main structural highs (A, B and C), clearly identifiable by local positive free-air gravity anomalies. These transverse normal faults define the step-like morphology of the Gulf of Cadiz, from the shelf to its outer parts (Figure 10).

[29] To the north of the basement high, Mesozoic to early Tertiary cover rocks show a gentle organization, with a regional dip to the southeast [Terrinha *et al.*, 2002]. They connect through a narrow synclinal basin with the folded and faulted Mesozoic to Paleocene units imaged in the GC1 and GC3 MCS profiles (Figures 3 and 4b). The SE vergent folds and thrusts are parallel to the trend of the basement high (Figure 10). South of the basement high, the thrusting geometries of the fold and thrust belt units (i.e., Campo de Gibraltar Flysch) are arranged following arc-shaped boundaries (Figure 10). During the NW propagation of the allochthonous units the basement high probably acted as a tectonic barrier. This is suggested by the successive embayments along the front of the Guadalquivir Allochthonous unit, locally overriding the Guadalquivir fault (Figure 10).

[30] In the outer part of the Gulf of Cadiz, in the proximity of the Horseshoe Abyssal Plain, the edge of the Giant Chaotic Body was identified (Figure 10). The Giant Chaotic Body consists of homogeneous units, continuous for tens of kilometers, with a size and volume comparable to chaotic prisms occurring in orogenic belts [Torelli *et al.*, 1997]. The Giant Chaotic Body differs from the Guadalquivir Allochthonous unit, in that it lacks any thrust geometries and the contact with surrounding units is stratigraphic (“pinch out”) (Figure 10).

5.2. Timing of the Gulf of Cadiz Contraction: Emplacement of Large Allochthonous Masses

[31] During the Neogene evolution of the Betic-Rif Cordillera, mostly controlled by a regional N-S compres-

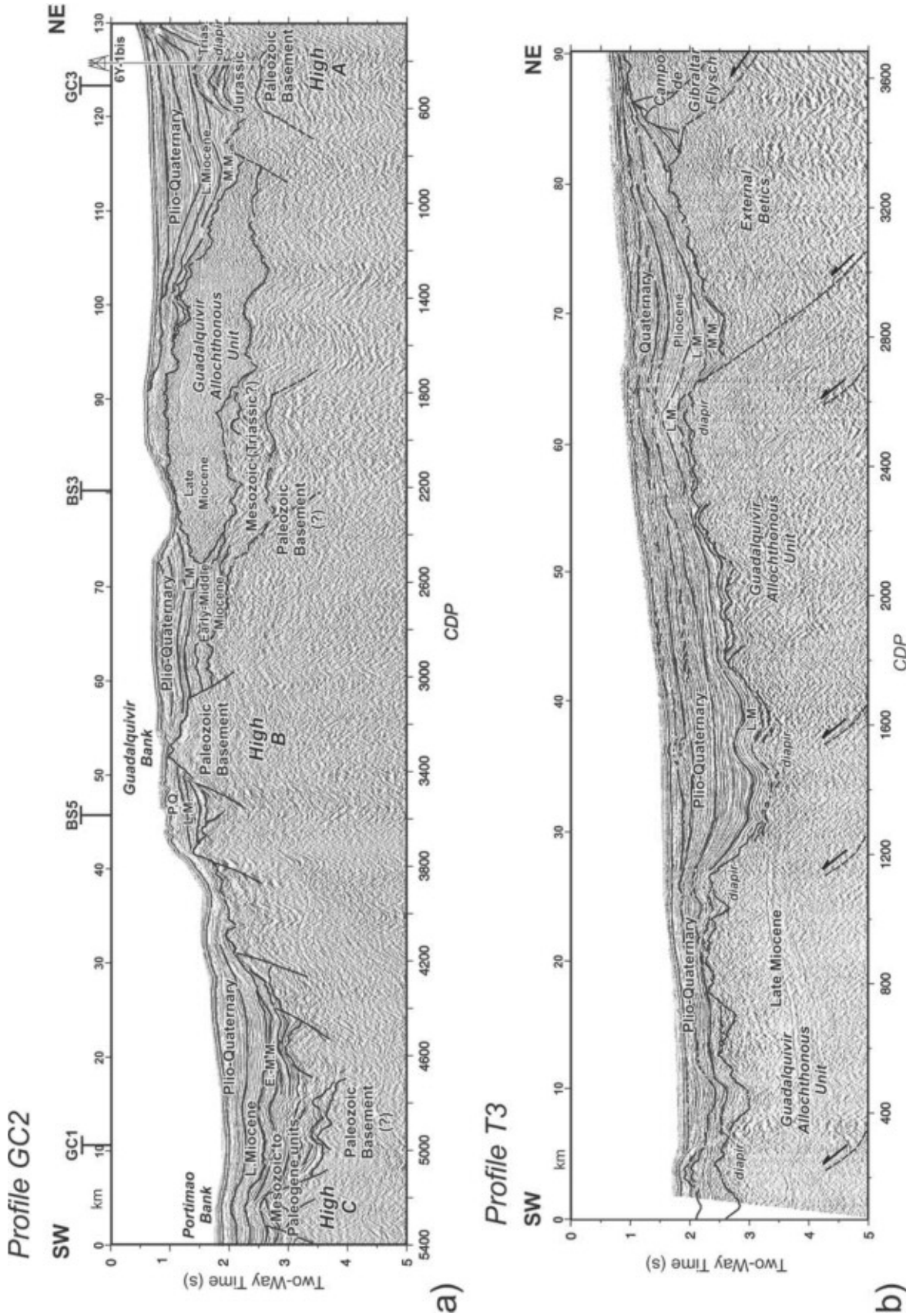


Figure 8. (a) Interpreted section of MCS line GC2, running along the highest values of the GCGH anomaly. Three structural highs (A, B, and C) are distinguished. (b) Interpreted MCS profile T3, located in the outer part of the Gulf of Cadiz. Trias: Triassic; E-MM: Early Middle Miocene; MM: Middle Miocene; LM: Late Miocene; PQ: Plio-Quaternary. See color version of this figure at back of this issue.

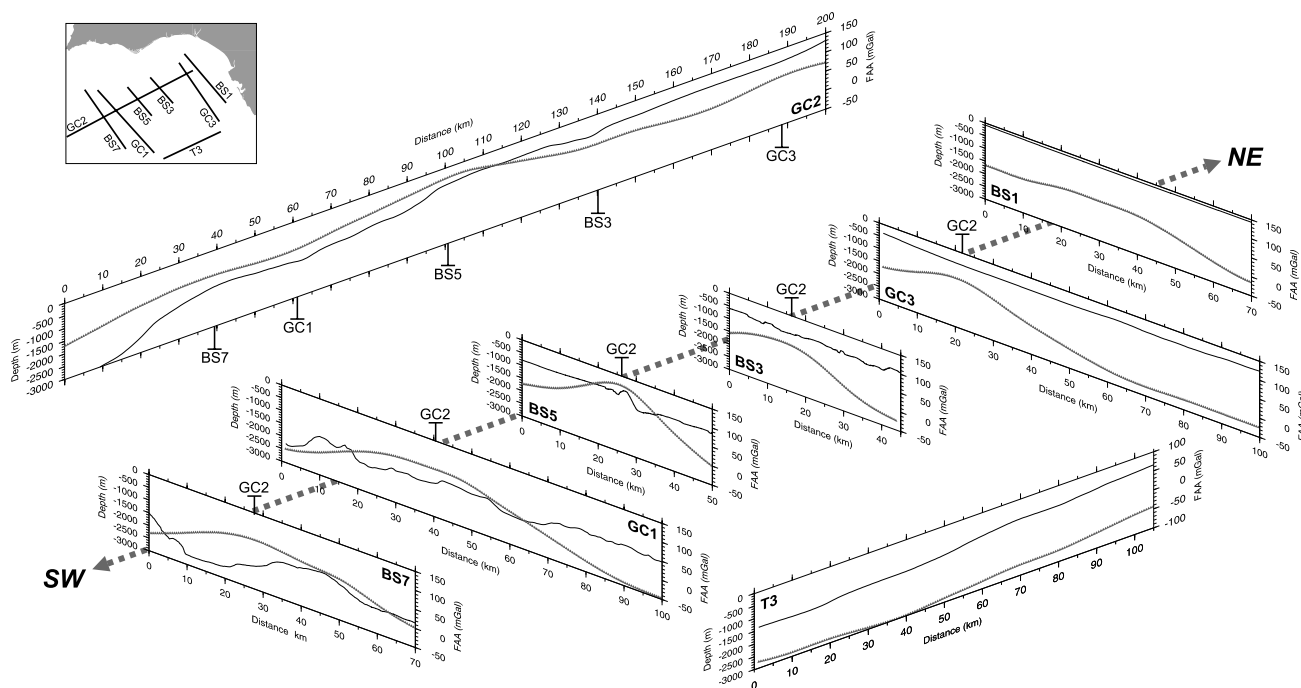


Figure 9. Bathymetry (thin lines) and free-air gravity anomaly (thick lines) profiles extracted along each MCS profiles of the Gulf of Cadiz (see location on small map). Profile GC2, which would be located along the thick dashed line, has been shifted to the upper part of the figure for clarity. FAA scale ranges between -50 and 150 mGal except for profile T3, which ranges between -100 and 100 mGal. Gravity data extracted from the gridded satellite database of *Sandwell and Smith [1997]*.

sion, the frontal sector of the Gibraltar Arc began to expel materials, in a radial, wedge-like movement, from their internal zones toward the present-day Gulf of Cadiz [*Andrieux et al., 1971; Sanz de Galdeano, 1990*]. These concentric wedges of folds and thrust belts, offshore continuation of the structural domains of the western Betics (Campo de Gibraltar, External Betics and Guadalquivir Allochthonous), were identified on the MCS lines across the shelf and upper slope of the Gulf of Cadiz. All of them show NW trending growth anticlines and synclines showing younger ages of deformation toward the foreland (Figure 11a), as also observed in seismic lines onshore and on the Gulf of Cadiz shelf [*Flinch et al., 1996; Berástegui et al., 1998; Maldonado et al., 1999*].

[32] The timing of emplacement of these tectonic units is determined by the crosscutting relationships between the structures and sedimentary deposits, calibrated by several nearshore oil wells. The emplacement of the Guadalquivir Allochthonous unit ended in the late Miocene (late Tortonian) (Figure 4a). Toward the southeastern end of the shelf, the External Betics are composed of Upper Cretaceous units. According to the gentle folding of the overlying Neogene units, their emplacement should be pre-Langhian (16 Ma). The Campo de Gibraltar unit, which is composed of flysch sequences and diapiric structures, shows a gentle northwest tilting of the upper sedimentary infill. In summary, we suggest a migration toward the northwest for the age of their final emplacement, from pre-early Langhian (16 Ma)

for the Campo de Gibraltar and External Betics, to late Tortonian (7–8 Ma) for the Guadalquivir Allochthonous unit (Figure 11b).

[33] The Neogene and Quaternary stratified sedimentary units of the Gulf of Cadiz shelf preserve the original topography of the system after the emplacement of the outermost allochthonous units (Figures 4 and 11a). In the MCS sections, we observe a differential topography between the front of the Guadalquivir Allochthonous and the Campo de Gibraltar units, suggesting that in late Tortonian, the Campo de Gibraltar units were close to sea level (Figures 8b and 11a). Deformation continued after late Tortonian, as is evidenced by a general tilt of the Plio-Quaternary stratified units toward the northwest, and by younger folding of the entire thrust system (Figure 11a). A rapid change in relative sea level, resulting from a vertical tectonic motion in the rear part of the thrust wedge and/or eustatic change, may have uplifted the platform of the Campo de Gibraltar above sea level. This has important implications given that it would have created a continuous passage across the Gibraltar Strait, allowing a faunal exchange between Africa and Iberia as suggested by paleomagnetic and biostratigraphic data [*Benammi et al., 1996; Garcés et al., 1998; Krijgsman et al., 2000*].

[34] Two possible mechanisms of emplacement of the Guadalquivir Allochthonous unit have been suggested. A tectonic emplacement, as an accretionary wedge of material carried above a thrust toward the foreland [e.g., *Flinch et al.,*

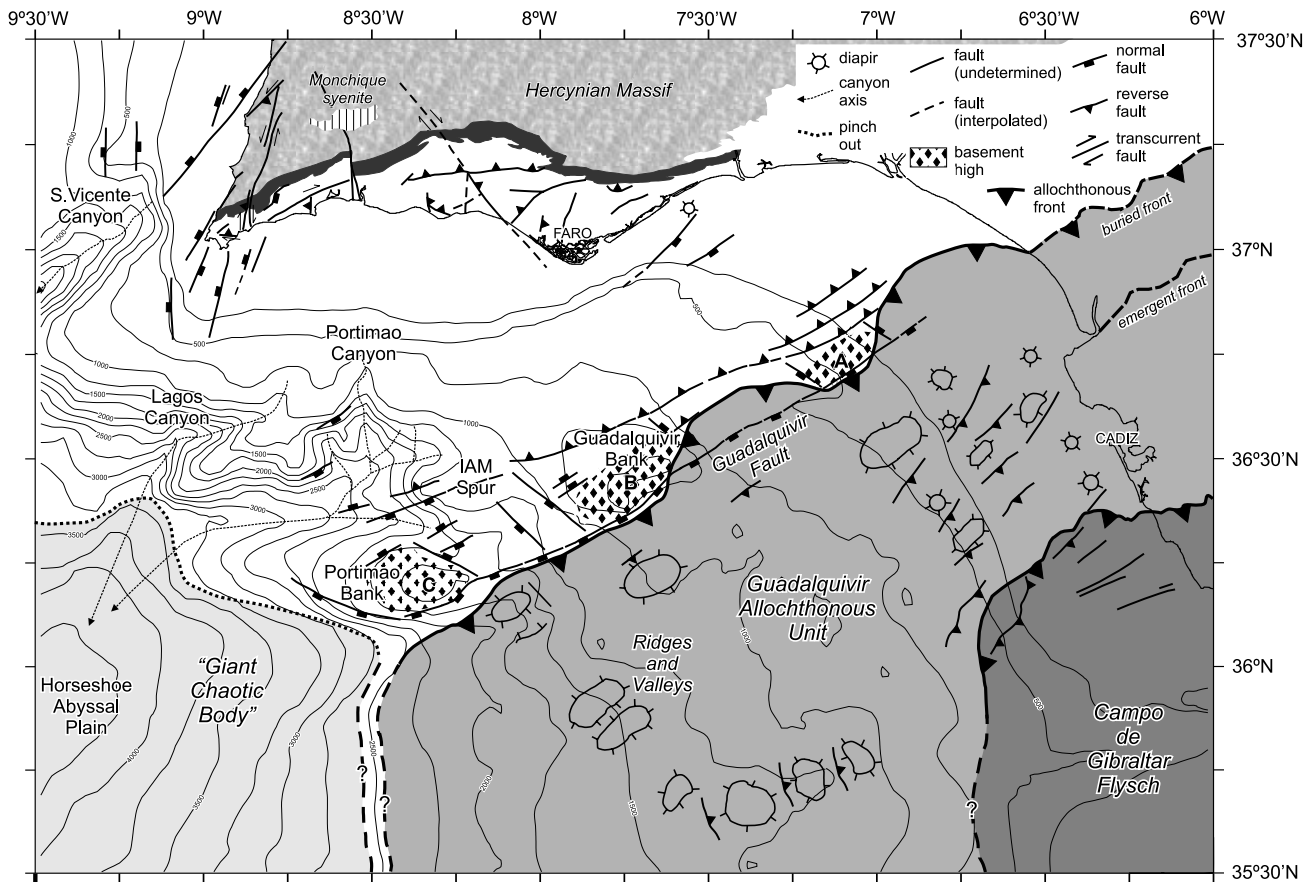


Figure 10. Interpretative structural map of the Gulf of Cadiz based on the results from MCS lines, together with gravity and high-resolution acoustic data. Information from earlier marine surveys has also been integrated [Baldy *et al.*, 1977; Torelli *et al.*, 1997; Maldonado *et al.*, 1999]. Tectonic map from the Algarve region (South Portugal) is summarized from Terrinha [1998] and Dias and Cabral [2000]. Fronts of the Guadalquivir Allochthonous onland are from Berástegui *et al.* [1998].

1996; Maldonado and Nelson, 1999; Maldonado *et al.*, 1999; Somoza *et al.*, 1999]; or by a lateral diapiric emplacement of Triassic evaporites, extruded by the tectonic load of thrust sheets directed toward the foreland [Berástegui *et al.*, 1998]. This last mechanism would imply intermixing tectonic intrusions of salt into Miocene marine sediments, and the subsequent disruption and folding of these allochthonous units by the continuous advancing of the thrusts. This last hypothesis is more in agreement with our observations on the Gulf of Cadiz MCS profiles: The Guadalquivir Allochthonous unit shows Triassic salt diapirs at its front (Figure 4a) and, probably, as detachment levels, along its base. Previous to the emplacement of the Guadalquivir Allochthonous unit, large gravitational accumulations and submarine landslides formed the Giant Chaotic Body [e.g., Lajat *et al.*, 1975; Bonnin *et al.*, 1975; Torelli *et al.*, 1997].

5.3. Deep Crustal Structure of the Gulf of Cadiz: Gravity Modeling

[35] To constrain the crustal and upper mantle structure under the Gulf of Cadiz, a simple 2-D model of free-air

gravity anomaly was calculated (Figure 12). In this case, two-dimensional models are adequate due to the linear and elongated character of the free-air gravity anomalies observed in the region (Figure 1c). We modeled a NW-SE profile extending 220 km from the Algarve coast to offshore Morocco, across the basement high of the Gulf of Cadiz (Figures 1c and 12). The geometry of the sedimentary units and the top of the basement is based on the interpretation of MCS profile GC1 (Figure 7) and completed with regional data [Terrinha *et al.*, 2002]. The Moho depth and geometry of the lower units from the Algarve coast to the center of the Gulf of Cadiz is tied to the results of wide-angle seismic data [González *et al.*, 1996, 1998] and to the preliminary gravity and magnetic models presented by Dañobeitia *et al.* [1999].

[36] The sediments overlying the basement were modeled as two layers: Quaternary and Neogene upper sediments, comprising the Guadalquivir Allochthonous unit; and lower sediments, composed of the Paleogene and Mesozoic age strata. The average interval velocity and density of the sediments and crust was determined from wide-angle seismic modeling: 2000 kg/m³ for the upper sediments, 2300 kg/m³ for the lower sediments, 2700 kg/m³ for the

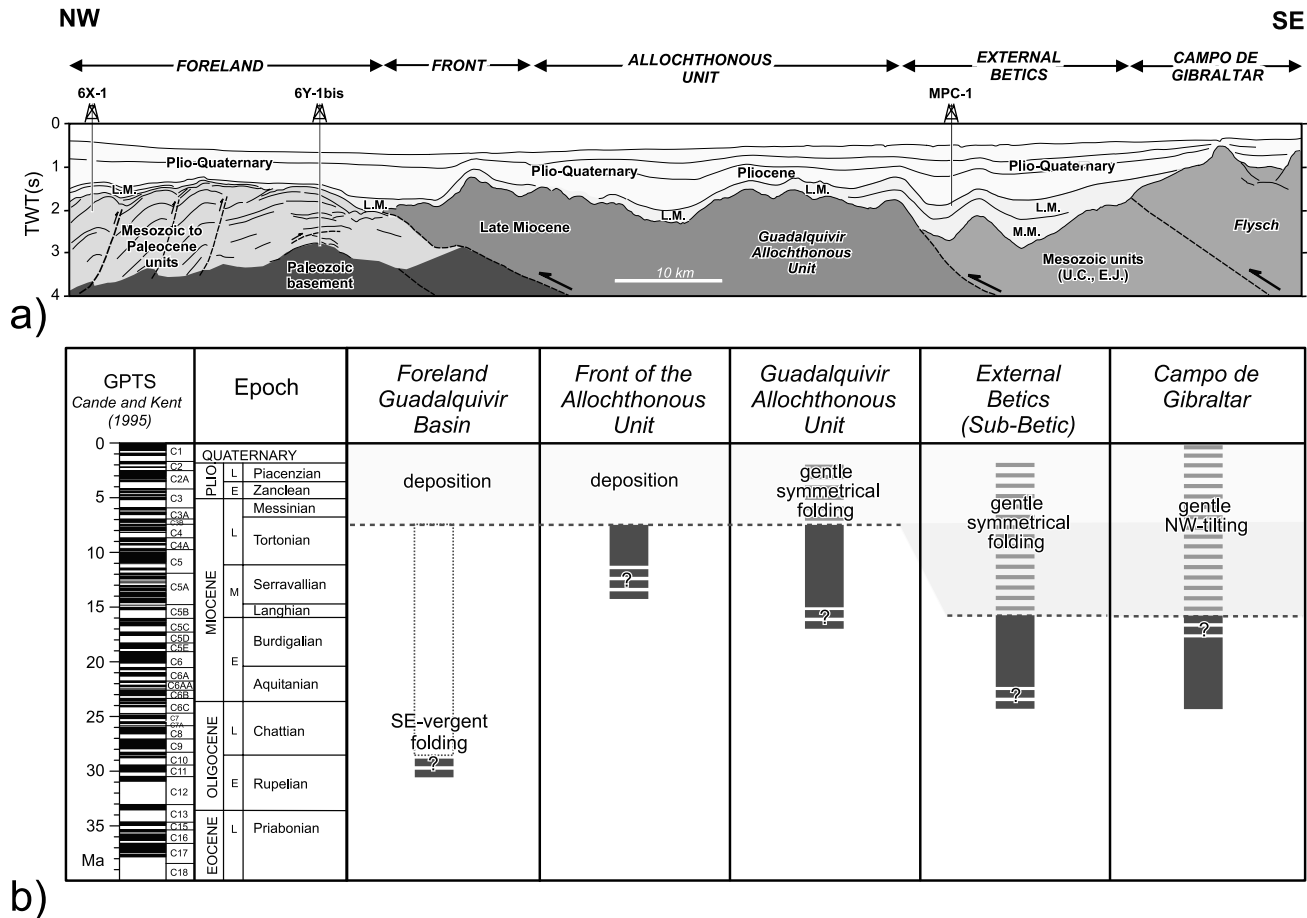


Figure 11. (a) Line drawing interpretation of the entire MCS profile GC3, with the location of the main structural units identified: Campo de Gibraltar, External Betics, Guadalquivir Allochthonous unit and front, and Foreland. EJ: Early Jurassic; UC: Upper Cretaceous; MM: Middle Miocene; LM: Late Miocene. TWT: two-way time. (b) Timing of emplacement of the aforementioned structural units. GPTS: geomagnetic polarity timescale [Cande and Kent, 1995]. See text for explanation.

upper crust, 2800 kg/m^3 for the middle crust, and 2950 kg/m^3 for the lower crust [González *et al.*, 1996, 1998]. The upper mantle was assigned a density of 3300 kg/m^3 .

[37] Figure 12a shows the best fit gravity model. The root mean square misfit between the observed and calculated anomalies is 3 mGal. A crustal thickness of about 21 km is suggested for the central part of the Gulf of Cadiz. This value is significantly lower than those obtained for the Algarve shelf and Moroccan margin (30 km). A relative ascent of the Moho boundary of up to 10 km is supported by the gravity model (Figure 12b). The crustal thinning underneath the Gulf of Cadiz basement high would have been generated during the Mesozoic extensional phase, generation the narrow and elongated high, which corresponds to the observed GCGH anomaly.

5.4. Evolution of the Africa-Eurasian Plate Boundary Within the Gulf of Cadiz

[38] The Gulf of Cadiz has undergone successive deformation phases corresponding to the evolution of the Afri-

can, Iberian, and Eurasian plate boundaries since the initial rifting of the North Atlantic [e.g., Olivet, 1996] (Figure 13a). In the last 10 years, different plate kinematic models have been proposed for the North Atlantic region [Mauffret *et al.*, 1989; Malod and Mauffret, 1990; Srivastava *et al.*, 1990; Roest and Srivastava, 1991; Olivet, 1996]. Although most authors agree on locating the major tectonic events, only a few of them provide sufficient detail of the evolution of the Iberian plate within the global setting [e.g., Olivet, 1996]. Our results will be related to this kinematic evolution.

[39] On the basis of identification of aeromagnetic anomalies, Srivastava *et al.* [1990] suggested that there has been a model of jumping plate boundary between Eurasia and Africa since anomaly M0 (120 Ma). For the older period, late Jurassic to Lower Cretaceous, Mauffret *et al.* [1989] and Malod and Mauffret [1990] on the basis of geological evidence predicted an oblique opening between Iberia and Africa (Figure 13a). A broad transform zone involving transcurrent faults with opening of pull-apart basins controlled the formation of the South Iberian and

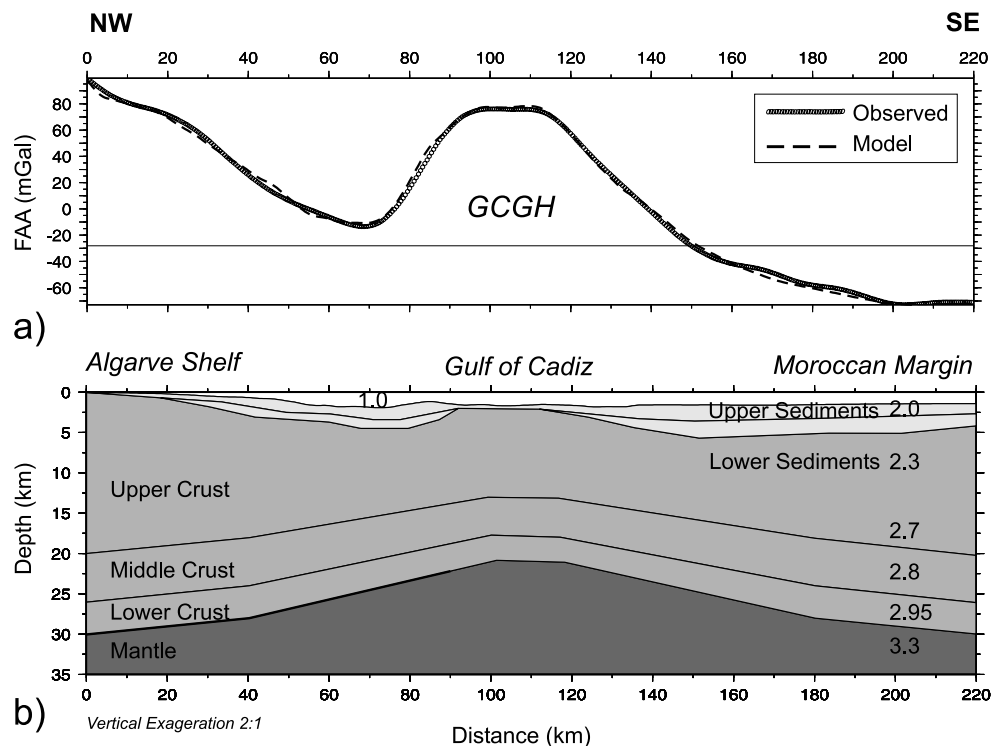


Figure 12. Two-dimensional gravity model from the Algarve to the Moroccan Margin, across the Gulf of Cadiz Gravity High (GCGH) (see Figure 1c for location). (a) Observed and calculated free-air gravity anomalies. (b) Best fit gravity model. In bold line, section constrained by wide-angle modeling [González *et al.*, 1996].

North African margins (Figure 13aI). During the Lower Cretaceous episode (Valanginian to Aptian), their model predicts a N-S extension, with the development of deep basins between North Africa and Iberia (Figure 13aII). We suggest that the extensional architecture of Gulf of Cadiz (the NE-SW step-like morphology and NW-SE structural highs alignment, together with a localized crustal thinning along the center of the Gulf) could have first developed during this period (Figure 13bI). The sharp boundaries limiting the basement high could be related to transform faults of transcurrent motion defining the original rift segmentation. In contrast to a number of authors [e.g., *Flinch et al.*, 1996; *Maldonado et al.*, 1999], we did not find any geological or geophysical evidence of oceanic crust being generated at this stage.

[40] At Chron 34 (Santonian, 84 Ma), Iberia was attached to the African plate and the plate boundary with Eurasia was then located at the Bay of Biscay [*Srivastava et al.*, 1990], when Alpine compression started to generalize [*Olivet*, 1996]. The compressional phase at the Gulf of Cadiz, may have started as early as late Paleocene (Chron 24, 56 Ma) (Figure 13aIII), as evidenced by the pre-Neogene folding of the foreland units in the MCS profiles (Figures 4b and 10). The Azores-Gibraltar fracture zone has been the plate boundary between Africa and Iberia since Chron 18 although the relative motion was small until early Oligocene (Chron 13, 36 Ma). Since then, the motion has been extensional near the Azores, strike slip along the

Gloria fault and compressional east of Gorringe Ridge [*Roest and Srivastava*, 1991] (Figure 13aIV).

[41] The evolution of the Gulf of Cadiz since Chron 6 (20 Ma) has been dominated by a regional N-S compression, by the subduction of the African plate under the South Sardinian Domain, and by the opening of the Algerian-Provençal basin during the early and middle Miocene [*Andrieux et al.*, 1971; *Sanz de Galdeano*, 1990]. These factors caused the closing of the Western Mediterranean area and the lateral expulsion of the Internal Zones of the Betic and Rif Cordilleras toward the west and WSW (see section 5.1) (Figure 13aIV). During the Tortonian, the main direction of compression began to rotate toward the NNW-SSE [i.e., *Sanz de Galdeano*, 1990], and, as evidenced on the MCS profiles and structural map (Figure 10), large allochthonous units and gravitational accumulations were emplaced toward the Gulf of Cadiz (Figure 13bII). The distribution of these units was controlled by the preexisting extensional structures.

[42] Compressional and strike-slip focal mechanisms and widespread seismicity registered in the area provide evidence of a WNW convergence in the Gulf of Cadiz [*Argus et al.*, 1989; *Buform et al.*, 1988] (Figure 1b). Present-day deformation accommodated by faulting is mainly attributed to its associated processes, such as pockmarks and mass-wasting deposits. The Guadalquivir Fault, that bounds the SE flank of the basement high, appears as a high-angle normal fault near the surface. However, at depth it probably develops into a low-angle detachment merging with other

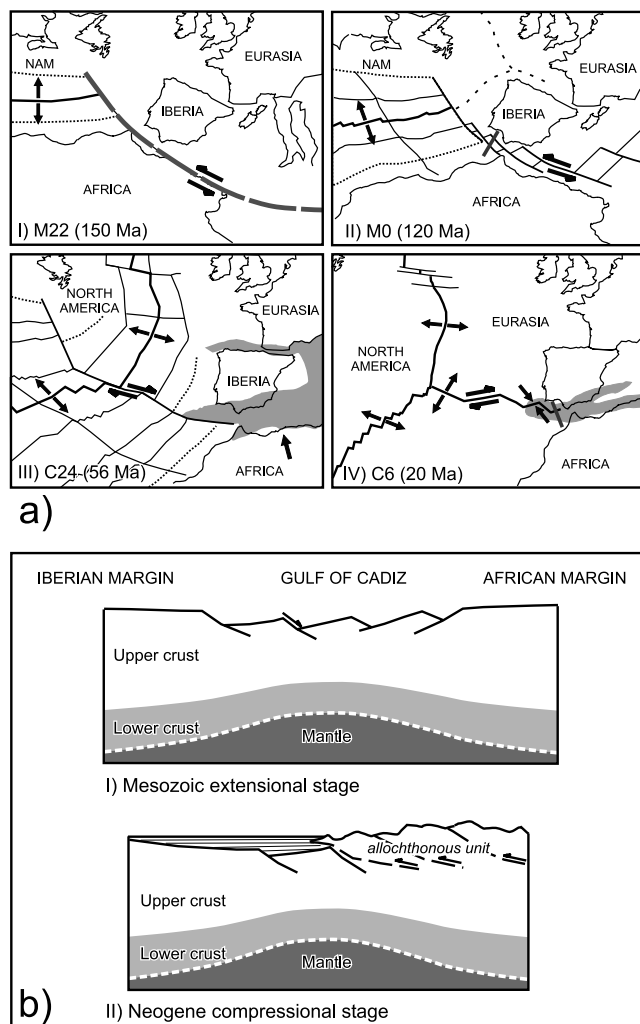


Figure 13. (a) Sketch of the kinematic evolution of the African, Iberian and Eurasian plates from M22, M0, Chron 24 and Chron 6. Gray depicts main compressional zones. (Modified from Olivet [1996]). (b) Simplified models of the Gulf of Cadiz evolution: (I) During the Mesozoic extensional stage (M0, 120 Ma), normal faulting and crustal thinning develops; (II) During the main Neogene compressional phase (C6, 20 Ma), faults are inverted, and large allochthonous masses are emplaced. Both sections are located in Figure 13a.

faults, as suggested by the intermediate seismicity (20–30 km) [e.g., Buforn et al., 1995; Seber et al., 1996]. These faults, such as the Guadalquivir Fault, correspond to weak areas inherited from the Mesozoic rifting phases. During the Cenozoic compressional phases they were probably reactivated and inverted, as suggested by tilting and deformation of sedimentary units.

6. Conclusions

[43] 1. The combined interpretation of multichannel seismic reflection profiles together with high-resolution ba-

thymetry, subbottom profiler, and gravity data allow us to gain insights into the tectonic architecture and crustal structure of the Gulf of Cadiz. The geometry of the seismostratigraphic units in the inner part of the Gulf clearly follows the main tectonic domains of the onshore western Betic Cordillera (Guadalquivir Allochthonous, External Betics and Campo de Gibraltar) (profiles BS1 and GC3). A similar geometry is found toward the middle and outer part of the Gulf of Cadiz (profiles BS3, BS5 and GC1), where the Paleozoic basement, Mesozoic cover and Miocene allochthonous units are shallower, with a thin Plio-Quaternary drape showing erosional features. The Paleozoic basement crops out at the Guadalquivir Bank, bounded by a large normal fault (Guadalquivir fault), which displaces the surrounding seafloor up to 500 m. Recent tectonic activity is observed on the Plio-Quaternary units around the bank.

[44] 2. The Gulf of Cadiz Gravity High (GCGH) anomaly is associated with a NE-SW trending basement high, its southern flank limited by a prominent normal fault (Guadalquivir fault). Imaged in detail, the basement high is composed of an alignment of three structural highs (A, B and C), one of them (B) locally outcropping at the Guadalquivir Bank. Two-dimensional-forward gravity modeling suggests that the elongated gravity high is also associated with crustal thinning of up to 10 km for the central part of the Gulf. All these extensional features (normal faulting and crustal thinning) were formed during the main Mesozoic rifting phase taking place between Iberia and Africa. It is during this phase that the original segmentation of the basin (i.e., sharp limits of the GCGH and basement high) could have occurred through transcurrent faulting.

[45] 3. During the Neogene convergence between the Iberian and African plates, several allochthonous units were emplaced. The age of the end of the deformation migrated toward the NW, from pre-early Langhian (16 Ma) (Campo de Gibraltar and External Betics) to late Tortonian (7–8 Ma) (Guadalquivir Allochthonous unit). Gentle symmetrical folding, probably generated by diapiric uplift, affects the Neogene units at the back of the allochthonous front. The Neogene units located in the foreland basin appear undisturbed, fossilizing an erosional post-Oligocene paleotopography. Large mass-wasting deposits, such as the Giant Chaotic Body, were emplaced as far as the Horseshoe Abyssal Plain.

[46] 4. Present-day convergence between the Eurasian and African plates, suggested by focal mechanisms and seismicity, is evidenced by active faulting and associated processes (seafloor surface ruptures, pockmarks and submarine landslides) taking place in the Gulf of Cadiz. However, the original extensional architecture of the Gulf was maintained through the different deformation phases. Thrusting geometries, suggested by compressional fault plane solutions recorded at depths between 14 and 30 km are probably accommodated by the reactivation and inversion of Mesozoic extensional faults, such as the Guadalquivir fault.

[47] **Acknowledgments.** The authors are grateful for funding from the European Commission project BIGSETS (ENV4-CT97-0547), Spanish national projects MAIAE (MAR98-0962), SENSUAL (REN2000-1016-C02-MAR), MARSIBAL (REN2001-3868-C02-MAR) Comissionat per a

Universitats i Recerca - Generalitat de Catalunya, Ministerio de Educación y Cultura and Ministerio de Ciencia y Tecnología (to E. Gràcia), and NATO grant EST.CLG.978922 (to J. Vergés). We wish thank the captain, crew and scientists on board the R/V *Urania* and BIO *Hesperides* for their assistance throughout the data collection. We are indebted to M. Torné for kindly

providing the IAM project MCS data of the Gulf of Cadiz, and N. Zitellini chief scientist of the BIGSETS 98 cruise. We thank R. Pallàs, A. M. Negro, J. L. Olivet, and an anonymous reviewer for helpful suggestions and comments. The Department of Geophysics (ICTJA-CSIC) is a Grup d'Excellència de Qualitat (ref. 2001 SGR 00339).

References

- Andrieux, J., J. M. Fontboté, and M. Mattauer, Sur un modèle explicatif de l'Arc de Gibraltar, *Earth Planet. Sci. Lett.*, **12**, 191–198, 1971.
- Argus, D. F., R. G. Gordon, C. DeMets, and S. Stein, Closure of the Africa-Eurasia-North America plate motion circuit and tectonics of the Gloria Fault, *J. Geophys. Res.*, **94**, 5585–5602, 1989.
- Auzende, J. M., J. L. Olivet, and L. Pastouret, Implications structurales et paléogéographiques de la présence de Messinien à l'Ouest de Gibraltar, *Mar. Geol.*, **43**, M9–M18, 1981.
- Baldy, P., G. Boillot, P. A. Dupeuble, J. Malod, I. Moita, and D. Mougénot, Carte géologique du plateau continental sud-portugais et sud-espagnol (Golfe de Cadix), *Bull. Geol. Soc. Fr.*, **XXIX**, 703–724, 1977.
- Banda, E., M. Torné, and Iberian Atlantic Margins Group, Iberian Atlantic Margins Group investigates deep structure of ocean margins, *Eos Trans. AGU*, **76**(3), 25, 28–29, 1995.
- Baraza, J., G. Ercilla, and H. C. Nelson, Potential geological hazards on the eastern Gulf of Cadiz slope (SW Spain), *Mar. Geol.*, **155**, 191–215, 1999.
- Benammi, M., M. Calvo, M. Prvot, and J. J. Jaeger, Magnetostratigraphy and paleontology of At Kandoula basin (High Atlas, Morocco) and the African-European late Miocene terrestrial fauna exchanges, *Earth Planet. Sci. Lett.*, **145**, 15–29, 1996.
- Berástegui, X., C. Banks, C. Puig, C. Taberner, D. Walthan, and M. Fernández, Lateral diapiric emplacement of Triassic evaporites at the southern margin of the Guadalquivir Basin, Spain, in *Cenozoic Foreland Basins of Western Europe*, edited by A. Mascle et al., *Geol. Soc. Spec. Publ.*, **134**, 49–68, 1998.
- Bergeron, A., and J. Bonnin, The deep structure of Gorringe Bank (NE Atlantic) and its surrounding area, *Geophys. J. Int.*, **105**, 491–502, 1991.
- Bonnin, J., J. L. Olivet, and J. M. Auzende, Structure en nappe à l'ouest de Gibraltar, *C. R. Acad. Sci. Paris, Ser. D*, **280**, 559–562, 1975.
- Bufo, E., A. Udías, and M. A. Colombas, Seismicity, source mechanisms and tectonics of the Azores-Gibraltar plate boundary, *Tectonophysics*, **152**, 89–118, 1988.
- Bufo, E., C. Sanz de Galdeano, and A. Udías, Seismotectonics of the Ibero-Maghreb region, *Tectonophysics*, **248**, 247–261, 1995.
- Cande, S. C., and D. V. Kent, Revised calibration of the geomagnetic polarity timescale for the late Cretaceous and Cenozoic, *J. Geophys. Res.*, **100**, 6093–6095, 1995.
- Dañoibeitia, J. J., R. Bartolomé, A. Checa, A. Maldonado, and A. P. Sloomweg, An interpretation of a prominent magnetic anomaly near the boundary between the Eurasian and African plates (Gulf of Cadiz, SW margin of Iberia), *Mar. Geol.*, **155**, 45–62, 1999.
- Delaplanche, J., Y. Lafet, B. G. Siñeriz, and M. A. Remon Gil, Seismic reflection applied to sedimentology and gas discovery in the Gulf of Cadiz, *Geophys. Prospect.*, **30**, 25–57, 1982.
- Dias, R. P., and J. Cabral, Evidências de paleoseismicidade na região do Algarve, paper presented at 2a Assembleia Hispano-Portuguesa de Geodesia y Geofísica, Inst. Geofís. Infante D. Luis de la Univ. de Lisboa, Lagos, Portugal, 8–12 Feb., 2000.
- Flinch, J. F., A. W. Bally, and S. Wu, Emplacement of a passive-margin evaporitic allochthon in the Betic Cordillera of Spain, *Geology*, **24**, 67–70, 1996.
- Frizon de Lamotte, D., J. Andrieux, and J. C. Guezou, Cinématique des chevauchements néogènes dans l'Arc bético-rifain: Discussion sur les modèles géodynamiques, *Bull. Geol. Soc. Fr.*, **162**, 611–626, 1991.
- Fukao, Y., Thrust faulting at a lithospheric plate boundary: The Portugal earthquake of 1969, *Earth Planet. Sci. Lett.*, **18**, 205–216, 1973.
- Garcés, M., W. Krijgsman, and J. Agustí, Cronology of the late Turolian deposits of the Fortuna basin (SE Spain): Implications for the Messinian evolution of the eastern Betics, *Earth Planet. Sci. Lett.*, **163**, 69–81, 1998.
- Gardner, J. M., Mud volcanoes revealed and sampled on the western Moroccan continental margin, *Geophys. Res. Lett.*, **28**(2), 339–342, 2001.
- González, A., M. Torné, D. Córdoba, N. Vidal, L. M. Matias, and J. Díaz, Crustal thinning in the Southwestern Iberian margin, *Geophys. Res. Lett.*, **23**(18), 2477–2480, 1996.
- González, A., D. Córdoba, R. Vegas, and L. M. Matias, Seismic crustal structure in the southwest of the Iberian Peninsula and the Gulf of Cadiz, *Tectonophysics*, **296**, 317–331, 1998.
- Gràcia, E., J. J. Dañoibeitia, J. Vergés, R. Bartolomé, and D. Córdoba, The structure of the Gulf of Cadiz (SW Iberia) imaged by new multi-channel seismic reflection data, paper presented at XXV General Assembly of the European Geophysical Society (EGS), Nice, France, 25–29 April, 2000.
- Gràcia, E., J. J. Dañoibeitia, and J. Vergés, Mapping active faults offshore Portugal (36°N–38°N): Implications for seismic hazard assessment along the southwest Iberian margin, *Geology*, **31**, 83–96, 2003.
- Grimison, N. L., and W. P. Chen, The Azores-Gibraltar plate boundary: Focal mechanisms, depths of earthquakes and their tectonic implications, *J. Geophys. Res.*, **91**, 2029–2047, 1986.
- Harrington, P. K., Formation of pockmarks by pore-water escape, *Geo. Mar. Lett.*, **5**(3), 193–197, 1985.
- Hayward, N., A. B. Watts, G. K. Westbrook, and J. Collier, A seismic reflection and GLORIA study of compressional deformation in the Gorringe Bank, eastern North Atlantic, *Geophys. J. Int.*, **138**, 831–850, 1999.
- Instituto Geográfico Nacional (IGN), Boletín de sismos próximos, report, Inst. Geogr. Nacional, Madrid, Spain, 1999.
- Kiratzi, A. A., and C. B. Papazachos, Active crustal deformation from the Azores triple junction to the Middle East, *Tectonophysics*, **243**, 1–24, 1995.
- Krijgsman, W., M. Garcés, J. Agustí, I. Raffi, C. Taberner, and W. J. Zachariasse, The “Tortonian salinity crisis” of the eastern Betics (Spain), *Earth Planet. Sci. Lett.*, **181**, 497–511, 2000.
- Lajat, D., B. Bijou-Duval, R. Gonnard, J. Letouzey, and E. Winnock, Prolongement dans l'Atlantique de la partie externe de l'Arc bético-rifain, *Bull. Soc. Geol. Fr.*, **XVII**, 481–485, 1975.
- Lanaja, J. M., A. Navarro, J. L. Martínez Abad, J. DelValle, L. M. Rios, J. Plaza, R. del Potro, and J. Rodríguez de Pedro, *Contribución de la Exploración Petrolífera al Conocimiento de la Geología de España*, 465 pp., Inst. Geol. y Min. de España, Madrid, 1987.
- Laughton, A. S., R. B. Whitmarsh, J. S. M. Rusby, M. L. Somers, J. Revie, and B. S. McCartney, A continuous east-west fault on the Azores-Gibraltar Ridge, *Nature*, **237**, 217–220, 1972.
- Lobo, F. J., F. J. Hernández-Molina, L. Somoza, J. Rodero, A. Maldonado, and A. Barnolas, Patterns of bottom current flow deduced from dune asymmetries over the Gulf of Cadiz shelf (southwest Spain), *Mar. Geol.*, **164**, 91–117, 2000.
- Maldonado, A., and H. C. Nelson, Interaction of tectonic and depositional processes that control the evolution of the Iberian Gulf of Cadiz Margin, *Mar. Geol.*, **155**, 217–242, 1999.
- Maldonado, A., L. Somoza, and L. Pallarés, The Betic orogen and the Iberian-African boundary in the Gulf of Cadiz: Geological evolution (central North Atlantic), *Mar. Geol.*, **155**, 9–43, 1999.
- Malod, J. A., and J. Didon, Étude géologique par sismique réflexion et carottage de roches du plateau continental de la baie de Cadix (Espagne), *C. R. Acad. Sci. Paris, Ser. D*, **280**, 149–152, 1975.
- Malod, J. A., and A. Mauffret, Iberian plate motions during the Mesozoic, *Tectonophysics*, **184**, 261–278, 1990.
- Malod, J. A., and D. Mougénot, L'histoire géologique néogène du Golfe de Cadix, *Bull. Soc. Geol. Fr.*, **XXI**, 603–611, 1979.
- Mauffret, A., D. Mougénot, P. R. Miles, and J. A. Malod, Results from the Multichannel Reflection Profiling of the Tagus Abyssal Plain (Portugal): Comparison with the Canadian margin, in *Extensional Tectonics and Stratigraphy of the North Atlantic Margins*, edited by A. J. Tankard and H. R. Balkwill, *AAPG Mem.*, **46**, 379–393, 1989.
- Mendes-Victor, L., A. Ribeiro, D. Córdoba, S. Persoglia, G. Pellis, R. Sartori, L. Torelli, N. Zitellini, and J. J. Dañoibeitia, BIGSETS: Big sources of earthquakes and tsunamis in SW Iberia, *Eos Trans AGU*, **80**(46), Fall Meet. Suppl., F932, 1999.
- Mezcua, J., and J. Rueda, Seismological evidence for a delamination process under the Alboran Sea, *Geophys. J. Int.*, **129**, F1–F8, 1997.
- Minster, J. B., and T. H. Jordan, Present-day plate motions, *J. Geophys. Res.*, **83**, 5331–5354, 1978.
- Nelson, C. H., and A. Maldonado, The Cadiz margin study off Spain: An introduction, *Mar. Geol.*, **155**, 3–9, 1999.
- Nelson, C. H., J. Baraza, and A. Maldonado, Mediterranean undercurrent sandy contourites, Gulf of Cadiz, Spain, *Sediment. Geol.*, **82**, 103–131, 1993.
- Olivet, J. L., La cinématique de la Plaque Ibérique, *Bull. Cent. Rech. Elf Explor. Prod.*, **20**, 131–195, 1996.
- Ribeiro, A., J. Cabral, R. Baptista, and L. Matias, Stress pattern in Portugal mainland and the adjacent Atlantic region, West Iberia, *Tectonics*, **15**(2), 641–659, 1996.
- Roberts, D. G., The Rif-Betic orogen in the Gulf of Cadiz, *Mar. Geol.*, **9**, 31–37, 1970.
- Rodero, J., L. Pallarés, and A. Maldonado, Late Quaternary seismic facies of the Gulf of Cadiz Spanish margin: Depositional processes influenced by sea-level change and tectonic controls, *Mar. Geol.*, **155**, 131–156, 1999.
- Roest, W. R., and S. P. Srivastava, Kinematics of the plate boundaries between Eurasia, Iberia and Africa in the North Atlantic from the Late Cretaceous to the present, *Geology*, **19**, 613–616, 1991.
- Sandwell, D. T., and W. H. F. Smith, Gravity anomaly from Geosat and ERS1 satellite altimetry, *J. Geophys. Res.*, **102**, 10,039–10,054, 1997.

- Sanz de Galdeano, C., Geologic evolution of the Betic Cordilleras in the Western Mediterranean, Miocene to present, *Tectonophysics*, 172, 107–119, 1990.
- Sartori, R., L. Torelli, N. Zitellini, D. Peis, and E. Lodolo, Eastern segment of the Azores-Gibraltar line (central-eastern Atlantic): An oceanic plate boundary with diffuse compressional deformation, *Geology*, 22, 555–558, 1994.
- Seber, D., M. Barazangi, A. Ibenbrahim, and A. Demnati, Geophysical evidence for lithospheric delamination beneath the Alboran Sea and Rif-Betic mountains, *Nature*, 379, 785–790, 1996.
- Somoza, L., A. Maestro, and A. Lowrie, Allochthonous blocks as hydrocarbons traps in the Gulf of Cadiz, paper presented at 1999 Offshore Technology Conference, Houston, Tex., 1999.
- Souriau, A., Geoid anomalies over Gorringe Ridge, North Atlantic Ocean, *Earth Planet. Sci. Lett.*, 68, 101–114, 1984.
- Srivastava, S. P., H. Schouten, W. R. Roest, K. D. Klitgord, L. C. Kovacs, J. Verhoef, and R. Macnab, Iberian plate kinematics: A jumping plate boundary between Eurasia and Africa, *Nature*, 344, 756–759, 1990.
- Terrinha, P., Structural geology and tectonic evolution of the Algarve Basin, South Portugal, Ph.D. thesis, 430 pp., Univ. College of London, London, UK, 1998.
- Terrinha, P., C. Ribeiro, J. C. Kullberg, C. Lopes, R. Rocha, and A. Ribeiro, Compressive episodes and faunal isolation during rifting, Southwest Iberia, *J. Geol.*, 110, 101–113, 2002.
- Torelli, L., R. Sartori, and N. Zitellini, The giant chaotic body in the Atlantic Ocean off Gibraltar: New results from a deep seismic reflection survey, *Mar. Pet. Geol.*, 14(5), 125–138, 1997.
- Tortella, D., M. Torné, and A. Pérez-Estaun, Geodynamic evolution of the eastern segment of the Azores-Gibraltar zone: The Gorringe Bank and the Gulf of Cadiz region, *Mar. Geophys. Res.*, 19, 211–230, 1997.
- Udías, A., A. Lopez Arroyo, and J. Mezcua, Seismotectonics of the Azores-Alboran region, *Tectonophysics*, 31, 259–289, 1976.
- Zitellini, N., L. Mendes-Victor, D. Córdoba, J. J. Dañobeitia, R. Nicolich, G. Pellis, A. Ribeiro, R. Sartori, L. Torelli, and BIGSETS Team, Source of the 1755 Lisbon earthquake and tsunami investigated, *Eos Trans. AGU*, 82(26), 285-290-291, 2001.

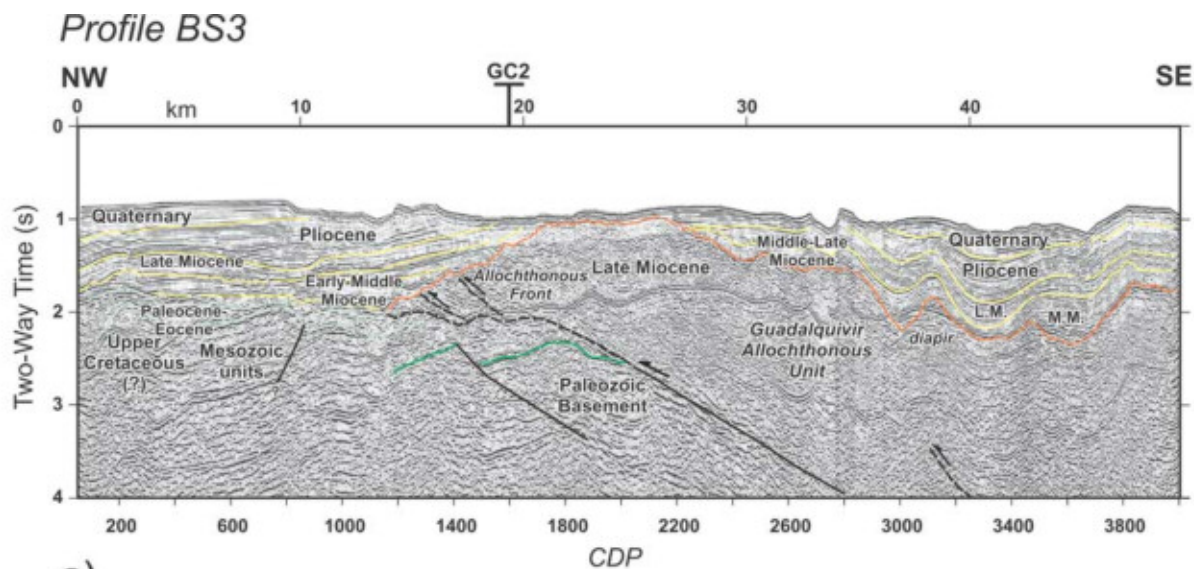
R. Bartolomé, Institut Universitaire Européen de la Mer, UMR 6538 Domaines Océaniques, Place Nicolas Copernic, F-29280 Plouzané, France. (Rafael.Bartolome@sdt.univ-brest.fr)

D. Córdoba, Departamento de Geofísica, Universidad Complutense de Madrid, E-28040 Madrid, Spain. (dcordoba@fis.ucm.es)

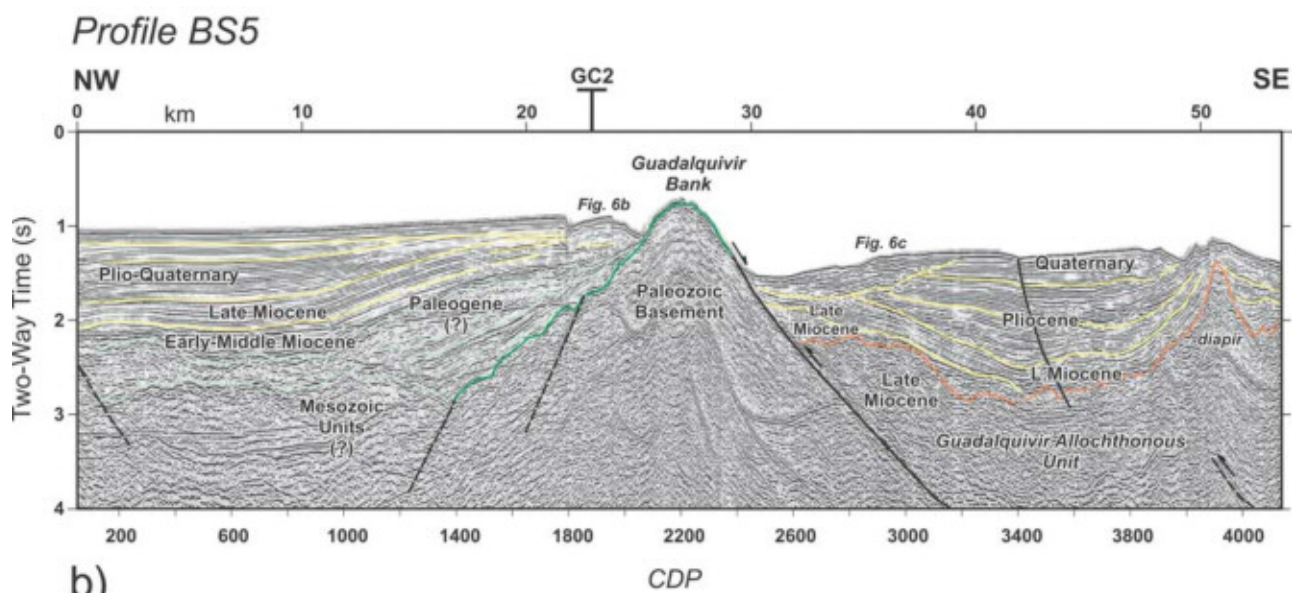
J. Dañobeitia and E. Gràcia, Unitat de Tecnologia Marina—CSIC, Centre Mediterrani d'Investigacions Marines i Ambientals (CMIMA), Passeig Marítim de la Barceloneta, 37-49, E-08003 Barcelona, Spain. (jjdanobeitia@utm.csic.es; egracia@utm.csic.es)

J. Vergés, Institut de Ciències de la Terra “Jaume Almera” (CSIC), Lluís Solé i Sabarís, E-08028 Barcelona, Spain. (jverges@ija.csic.es)

Figure 4. (opposite) (a) Interpreted MCS profiles BS1 and b) GC3. Both profiles are located along the Gulf of Cadiz shelf. MJ: Middle Jurassic; LC: Lower Cretaceous; UC: Upper Cretaceous; P: Paleocene; M: Miocene; CG Flysch: Campo de Gibraltar flysch. Paleozoic basement is depicted in dark green, Mesozoic to Paleogene units are in light green, and Neogene units in yellow. The Guadalquivir Allochthonous unit is depicted in red, and the Campo de Gibraltar and External Betics in brown. Faults are depicted in black, in dashed line when inferred. Same legend applies for Figures 5, 7, and 8.



a)



b)

Figure 5. (a) Interpreted MCS profiles BS3 and (b) BS5. Both profiles are located in the middle of the Gulf of Cadiz, around the Guadalquivir Bank. LM: Late Miocene; MM: Middle Miocene. Location of Figures 6b and 6c are depicted on profile BS5.

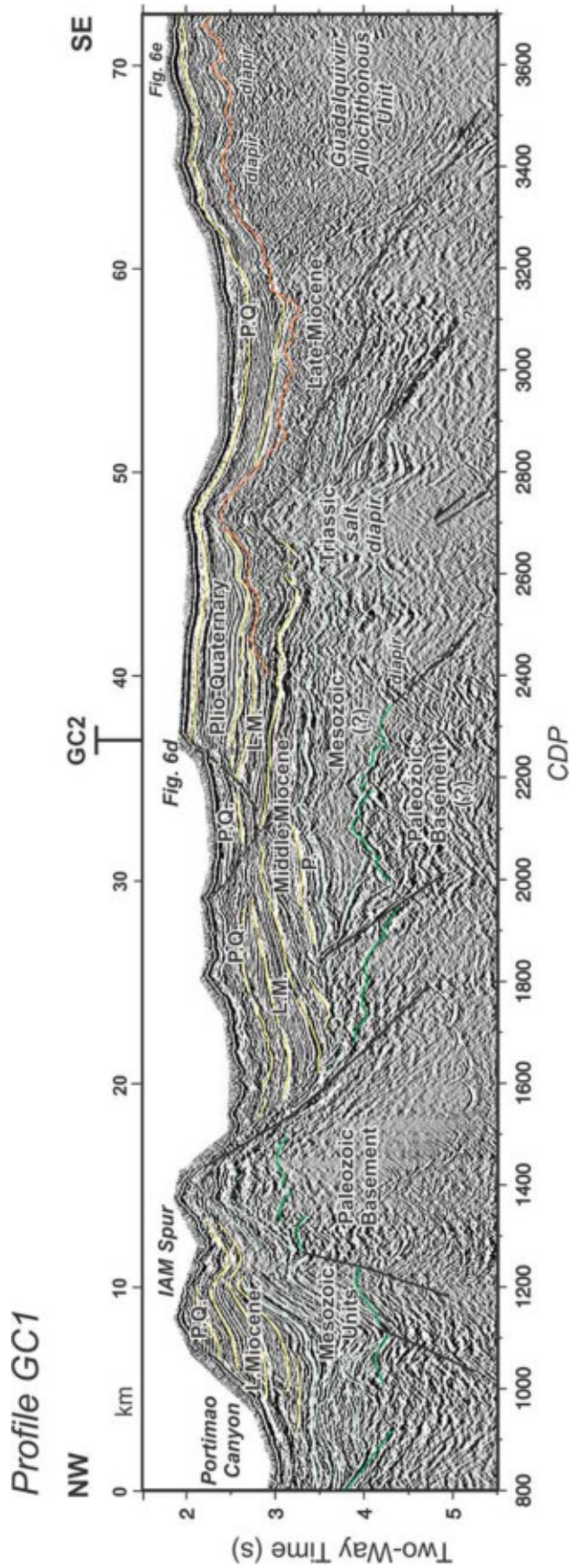


Figure 7. (opposite) Interpreted MCS profile GC1 in the outer part of the Gulf of Cadiz, south of the Portimao Canyon. P: Paleocene; LM: Late Miocene; PQ: Plio-Quaternary. Location of Figures 6d and 6e are depicted.

